A comprehensive distribution-free scheme for tri-aspect surveillance of complex processes

Abstract

Distribution-free charting schemes for process monitoring are more robust and reliable than their parametric counterparts when the process distributions are unknown and complicated. Most of the control charts are uni-aspect schemes because they can detect a shift in only one aspect of the process distribution, like location or scale. Research on schemes for simultaneous surveillance of location and scale parameters has been very active in recent years, leading to many bi-aspect schemes. These schemes do not explicitly deal with the shape of the process distribution. However, a shift in the shape parameter along with or without a location or scale shift can occur in practice, especially in production or time-to-event processes. Note that, there are nonparametric schemes for detecting general shifts based on goodness-of-fit test statistics, or empirical likelihood ratio statistics, which cannot isolate if there is a shift in location, scale, shape or some mixture of them. In this paper, we introduce a new distribution-free process monitoring scheme that can detect a shift in either of location, scale and shape parameters, or any combinations of them. The new scheme is based on a combined statistic designed via Euclidean distance of the standardized Wilcoxon statistic for location, the standardized Ansari-Bradley statistic for scale and the standardized Savage-type statistic for shape. We discuss the implementation design using the average run-length as the performance metric and investigate the in-control performance of the proposed scheme. It is shown that the new charting scheme is in-control robust irrespective to the underlying process distribution and therefore applicable to monitor any univariate continuous processes. An out-of-control performance comparison study of the new scheme with many existing schemes shows that the new scheme is preferable to the existing schemes, as none of them is designed to monitor the three process parameters simultaneously. We discuss an application of the new chart in monitoring arrival delays of a passenger train in a regional route in Italy. The proposed scheme is comprehensive in the sense that it integrates the follow-up procedure via integrated sub-charts for classifying the signalling component.

Keywords: Ansari-Bradley Statistic; Arrival Delay; Control Chart; Nonparametric Phase-II Analysis; Savage Statistics; Statistical Process Control; Wilcoxon Statistic.

1. Introduction

Quality 4.0 is one of the most critical aspects of the smart factory, where digitally enhanced processes increase productivity and flexibility in the factory and throughout the supply chain. Quality 4.0 emphasizes the crucial role of quality control in contributing to the smart factory evolution. Modern technologies and practices are used to improve overall quality, reduce supply chain interruptions, cost and time to market of products or service delivery. Quality 4.0 is a reference to Industry 4.0, the fourth industrial revolution promoted by the recent fast advancement in connectivity, mobility, scalability and data analytics. Industry 4.0 is resulting in transformations in manufacturing efficiency, supply chain performance, product innovation, and even entirely new business models. Quality 4.0 does not mean that traditional methods, like control charts, should be replaced but rather that they should be improved. Control charts play a central role in quality control and management because they are handy tools for improving the quality of a product, by limiting rework, slowdowns, and redundant processes.

Traditional control charts assume that the underlying process distribution has a known parametric form. For example, the Shewhart X-bar and R charts postulate that the process distribution is normal. Other familiar distributions that are assumed are the Exponential and Weibull ones. However, there are many situations where such assumptions are not met in practice. Examples are processes involved in monitoring service quality in a customer call centre or of bank teller counters, citizen satisfaction with municipal services, waiting time to reach a customer care executive or to get an appointment in a city hospital, punctuality of suburban rail services. Parametric control charts do not guarantee reliable results when their parametric assumptions on process distribution are not met. In this context, many scholars suggest the application of nonparametric, or distribution-free, control charts that are more robust and reliable than parametric charts because no parametric distributional assumption is required. Research on nonparametric control charts is very active. A search for “nonparametric control chart” OR “distribution-free control chart” in the past two decades shows that the interest is flourishing. Table 1 displays the number of search entries found in the most familiar academic databases.

Table 1. Search results for "nonparametric control chart" OR "distribution-free control chart"

Timespan	Google Scholar	Scopus	Dimension
Till 2000	57	26	50
2001-2005	49	11	41
2006-2010	95	69	100
2011-2015	222	178	336
2016-2020	381	404	606

Distribution-free charting schemes do not assume a specific distribution for the process, or just impose some general assumptions, such as continuous distribution or symmetric distribution. Therefore, the primary advantage of distribution-free charts over parametric counterparts is in-control (IC) robustness. The IC properties, such as IC average run-length (ARL_0) or false alarm rate (FAR) of these charts are invariant for all underlying process distributions. If the underlying process distribution is indeed normal, then distribution-free schemes may be slightly less efficient than parametric schemes. However, distribution-free schemes are markedly more efficient when the normality assumption is not met (Koutras, & Triantafyllou, 2018; Qiu, & Li, 2011; Qiu, & Zhang, 2015). Many distribution-free charts have been developed for location shifts (Balakrishnan, Triantafyllou, & Koutras, 2009; Chakraborti, Eryilmaz, & Human, 2009; Graham, Chakraborti, & Human, 2011; Graham, Mukherjee, & Chakraborti, 2012; Hawkins, & Deng, 2010; Li, Tang, & Ng, 2010; Abid, Nazir, Riaz, & Lin 2017), for scale shifts (Jones, & Champ, 2010; Zhou, Zhou, & Geng 2016), and for distribution changes (Ross, & Adams, 2012). See Chakraborti, van der Laan, & Bakir (2001); Qiu (2018); Chakraborti, & Graham (2019) for general accounts on distribution-free charts. We especially recommend reading Chapters 8 and 9 of Qiu (2014); and the book edited by Koutras, & Triantafyllou (2020).

Most of the traditional parametric and distribution-free control charts are either designed to monitor the location or the scale parameters separately. That is, one charting scheme is used for surveillance of one specific aspect of process quality. In practice, shifts in both the location and scale parameters of a process may happen simultaneously. Therefore, one chart for location and one for scale are often applied together. Rahim & Costa (2000) considered the economic design of the *X*-bar and *R* chart for monitoring both parameters of a normal distribution. David, & Grigoryan (2006) studied the joint statistical design of double sampling *X*-bar and *s* charts. Further, Zhang, Yang, Khoo, & Yu (2010) proposed an optimal design of control schemes for joint monitoring of mean and variance. Lee (2013) proposed the joint statistical design of *X*-bar and *s* charts with

combined double sampling and variable sampling interval. A serious disadvantage of using two separate control charts to monitor both the shift in location and variability is that monitoring becomes very complicated when a shift in one parameter affects the shift in the other parameter. Many scholars and practitioners advocated the introduction of schemes based on a single plotting statistic for jointly monitoring the location and scale parameters, leading to a very active research topic. Mukherjee, & Chakraborti (2012) first proposed a distribution-free Shewhart-Lepage (SL) scheme for jointly monitoring the location and scale parameters of a process that leads to a new dimension of research on bi-aspect monitoring. Subsquently, Chowdhury, Mukherjee, & Chakraborti (2015) proposed a cumulative sum scheme based on the Lepage statistic. Chowdhury, Mukherjee, & Chakraborti (2014) proposed a distribution-free Shewhart-Cucconi (SC) scheme for jointly monitoring the location and scale parameters of a process. Chong, Mukherjee, & Khoo (2017, 2018) respectively proposed a fuzzy monitoring scheme that combines two versions of the SL chart and a class of SL type schemes for one-sided joint monitoring. Mukherjee & Marozzi (2017a) introduced a circular-grid chart based on some Lepage-type statistics. Mukherjee, & Marozzi (2017b) and Mukherjee (2017) discussed respectively, some distribution-free cumulative sum ($CUSUM$) and exponentially weighted moving average ($EWMA$) schemes based on the Lepage statistic. A class of percentile modified SL type schemes was offered by Mukherjee, & Sen (2018). Zhang, Li, & Li (2017) proposed an $EWMA$ scheme based on the Cramér–von Mises test for joint monitoring of location and scale. Song, Mukherjee, Liu, & Zhang (2019) proposed two adaptive modifications of the SL chart. Other recent contributions to distribution-free location-scale joint monitoring schemes are Celano, Castagliola, & Chakraborti (2016); Li, Xie, & Zhou (2016); Song, Mukherjee, & Zhang (2020), Song, Mukherjee, Maozzi, & Zhang (2020), Mukherjee,& Marozzi (2020), among others.

A location-scale model cannot always precisely capture the true nature of the shift in the process distributions involving service quality or product reliability or general time-to-event because a shift in the underlying process can also happen in the shape parameter of the distribution. However, the largest share of the existing distribution-free charts consists of uni-aspect schemes monitoring either the location or the scale parameter only. A sizeable share of distribution-free charts has arisen more recently and consists of bi-aspect schemes for simultaneous monitoring of location and scale parameters. Motivated by the lack of schemes for simultaneous monitoring of location, scale and shape parameters, we propose in this paper a tri-aspect distribution-free chart.

Our idea is to modify the familiar bi-aspect Shewhart-Lepage scheme so that it is sensitive also to a shift in the shape parameter of the underlying process distribution. In this paper, we also use the idea of integrated sub-charts for comprehensive monitoring and follow-up to identify in which parameter the shift has actually happened. More precisely, in Section 2, we design the new chart by combining the Wilcoxon, Ansari Bradley and antisymmetric Savage statistics. In Section 3, we show how to implement the new chart. A performance comparison study with several multi-aspect charts is presented in Section 4. The application of the new chart to an actual problem is illustrated in Section 5. Section 6 concludes the paper with some remarks and a direction for further research.

2. The distribution-free tri-aspect scheme

Suppose that a random sample of size m is available from an IC process with an unknown univariate continuous distribution F_X. We recommend using an appropriate Phase-I analysis to establish it as a reference sample. Denote it by $\boldsymbol{X_m} = (X_1, \ldots, X_m)$. Let $\boldsymbol{Y_{j,n}} = (Y_{j1}, \ldots, Y_{jn})$ be the test sample obtained during the j^{th} stage of monitoring independently of $\boldsymbol{X_m}$. Suppose that test samples come from a univariate continuous distribution function denoted by G_Y. Kössler and Mukherjee (2020) introduced a versatile shift model, combining the general location-scale alternative and the Lehmann alternative as

$$G_Y(x) = \left[F_X\left(\frac{x-\theta}{e^{\vartheta}}\right)\right]^{e^{\delta}}, (\theta, \vartheta, \delta) \in \mathbb{R}^3,$$

where $\theta, \vartheta, \delta$ are respectively the location, scale and shape parameters. Equivalently, in a simplified notation, one may write

$$G_Y(x) = \left[F_X\left(\frac{x-\theta}{\vartheta'}\right)\right]^{\delta'}, \theta \in \mathbb{R}, \vartheta' \in \mathbb{R}^+, \delta' \in \mathbb{R}^+,$$

where θ is as before, ϑ' and δ' are the reparameterized scale and shape components, respectively. This form alternative allows flexibility to include various types of shifts, including classical isolated location, scale shift or Lehmann alternative as well as mixed location and scale shift as a particular case and is explained later.

We may note that the corresponding pdf is

$$g_Y(x) = \frac{\delta'}{\vartheta'} f_X\left(\frac{x-\theta}{\vartheta'}\right)\left[F_X\left(\frac{x-\theta}{\vartheta'}\right)\right]^{\delta'-1}, \theta \in \mathbb{R}, \vartheta' \in \mathbb{R}^+, \delta' \in \mathbb{R}^+,$$

For example, if $F_X\left(\frac{x-\theta}{\vartheta'}\right) = 1 - e^{-\frac{x-\theta}{\vartheta'}}$, $g_Y(x)$ is the pdf of an exponentiated shifted exponential random variable which includes popular exponentiated exponential, see Gupta and Kundu (2001), as a particular case when $\theta = 0$, if $F_X\left(\frac{x-\theta}{\vartheta'}\right) = \Phi\left(\frac{x-\theta}{\vartheta'}\right)$, Φ being the cdf of the normal distribution, we observe $g_Y(x)$ as exponentiated normal (EN) distribution as in Gupta and Gupta (2008). Note that a standard EN distribution is the same as the standard normal distribution. Further, the EN distribution with $\delta' = 2$ is the Azzalini's skew-normal distribution, see Li et al. (2019), for its uses SPM context. Exponentiated models of the form $g_Y(x)$ are widely addressed in modelling failure times, see, for example, Gupta et al. (1998) for some early reference.

Consider the null hypothesis $G_Y(x) = F_X(x)$, i.e. that the test sample and reference samples come from two identical populations, and no shift is involved. In symbols, it is

$$H_0\colon\ [\theta = 0, \vartheta = 0, \delta = 0]\ \equiv H_0\colon [\theta = 0, \vartheta' = 1, \delta' = 1].$$

Here, H_0 assumes that the process is IC. H_0 can be violated in several ways when the process is out-of-control (OOC). The pure location shift hypothesis corresponds to

$$G_Y(x) = F_X(x - \theta),$$

in symbols it is

$$H_l\colon\ [\theta \neq 0, \vartheta = 0, \delta = 0] \equiv \quad H_l\colon [\theta \neq 0, \vartheta' = 1, \delta' = 1].$$

The Wilcoxon statistic W can be used to test for this alternative hypothesis. The test does not require the assumption of normality and is the most standard nonparametric test. The Wilcoxon test is nearly as powerful as the Student t-test when the parent population is normal unless sample sizes are very small. In fact, the asymptotic relative efficiency (ARE) of the Wilcoxon test to the Student t-test is 0.955 under normal distributions. The ARE for the logistic, double exponential, uniform and exponential distributions are respectively 1.097, 1.5, 1.0, 3.0. In general, the ARE of the Wilcoxon test to the Student t-test has a lower bound of 0.864 but there is no upper bound, meaning that it can be infinitely more efficient than the Student t-test as emphasized by Lehmann (2009).

Consider the combined reference sample $\boldsymbol{X_m}$ and the j^{th} test sample $\boldsymbol{Y_{j,n}}$ of size N, where $N = m + n$ and sort its elements in the increasing order. Let λ_i be an indicator variable such that

$$\lambda_i = \begin{cases} 0 & \text{if the } i^{\text{th}} \text{ smallest element of the pooled sample belongs to } \boldsymbol{X_m}. \\ 1 & \text{otherwise} \end{cases}$$

The WI statistic for testing H_0 versus H_l is defined as

$$WI = \sum_{i=1}^{N} i\lambda_i.$$

The pure scale shift alternative hypothesis for process variability corresponds to

$$G_Y(x) = F_X\left(\frac{x}{e^{\vartheta}}\right) = F_X\left(\frac{x}{\vartheta'}\right),$$

in symbols, it is

$$H_v\colon [\theta = 0, \vartheta \neq 0, \delta = 0] \equiv H_v\colon [\theta = 0, \vartheta' \neq 1, \delta' = 1].$$

The Ansari-Bradley (AB) statistic can be used to test for this alternative hypothesis. The corresponding test does not require the assumption of normality and is quite familiar in practice being also featured, for example, in the standard textbook on nonparametric tests by Hollander, Wolfe, & Chicken (2013). Its ARE to the F test is 0.61 under normal distributions. The AB statistic for testing H_0 versus H_v is defined as

$$AB = \sum_{i=1}^{N} \left| i - \frac{N+1}{2} \right| \lambda_i.$$

The joint location-scale shift hypothesis corresponds to

$$G_Y(x) = F_X\left(\frac{x-\theta}{e^{\vartheta}}\right) = F_X\left(\frac{x-\theta}{\vartheta'}\right),$$

in symbols it is

$$H_{lv}\colon [\theta \neq 0, \vartheta \neq 0, \delta = 0] \equiv H_{lv}\colon [\theta \neq 0, \vartheta' \neq 1, \delta' = 1].$$

The Lepage statistic can be used to test for this alternative hypothesis. The corresponding test does not require the assumption of normality and is the most familiar test for this hypothesis in practice, see Hollander, Wolfe, & Chicken (2013). The Lepage statistic (LEP) is the sum of the squared standardized Wilcoxon statistic (L) for location and Ansari-Bradley statistic (V) for variability

$$LEP = \left(\frac{WI - \mu_{WI}}{\sigma_{WI}}\right)^2 + \left(\frac{AB - \mu_{AB}}{\sigma_{AB}}\right)^2 = L^2 + V^2,$$

where

$$\mu_{WI} = E(WI|H_0) = \frac{1}{2}n(N+1), \quad \sigma_{WI}^2 = Var(WI|H_0) = \frac{1}{12}mn(N+1);$$

$$\mu_{AB} = E(AB|H_0) = \begin{cases} \frac{nN}{4} & \text{if } N \text{ is even} \\ \frac{n(N^2-1)}{4N} & \text{if } N \text{ is odd} \end{cases},$$

and

$$\sigma_{AB}^2 = \ Var(AB|H_0) = \ \begin{cases} \frac{1}{48} mn \frac{(N^2-4)}{N-1} & \text{if } N \text{ is even} \\ \frac{1}{48} \frac{mn(N+1)(N^2+3)}{N^2} & \text{if } N \text{ is odd.} \end{cases}$$

Lepage (1971) showed that the Wilcoxon statistic and the Ansari-Bradley statistic are linearly uncorrelated under the null hypothesis. The LE statistic is the square of the Euclidean distance of (L, V) from (0,0).

The Lehmann alternative responsible for a shift in shape is quite familiar in reliability and survival analysis and corresponds to a shift in the shape parameter. It assumes that

$$G_Y(x) = [F_X(x)]^{e^\delta} = [F_X(x)]^{\delta'}.$$

In symbols, it is

$$H_s\colon\ [\theta = 0, \vartheta = 0, \delta \neq 0] \ \equiv \ H_s\colon\ [\theta = 0, \vartheta' = 1, \delta' \neq 1].$$

The Savage-type test statistic (SA) can be used to test for the Lehmann alternative, where

$$SA = \sum_{i=1}^{N} \left(1 - \sum_{j=i}^{N} \frac{1}{j}\right) \lambda_i.$$

The mean and variance of the SA statistic when the process is IC are respectively

$$\mu_{SA} = E(SA|IC) = 0 \text{ and } \sigma_{SA}^2 = Var(SA|IC) \ = \ \sqrt{\frac{mn}{N-1}\left(1 - \frac{1}{N}\sum_{j=1}^{N} \frac{1}{j}\right)}.$$

In various lifetime distributions and business and economic models, one may encounter OOC situations that are more complex than those outlined before. They are the location-shape shift corresponding to

$$H_{ls}\colon [\theta \neq 0, \vartheta = 0, \delta \neq 0] \ \equiv \ H_{ls}\colon\ [\theta \neq 0, \vartheta' = 1, \delta' \neq 1],$$

the variability-shape shift corresponding to

$$H_{vs}\colon [\theta = 0, \vartheta \neq 0, \delta \neq 0] \ \equiv \ H_{vs}\colon\ [\theta = 0, \vartheta' \neq 1, \delta' \neq 1],$$

or the versatile shift in location-variability-shape corresponding to

$$H_{lvs}\colon [\theta \neq 0, \vartheta \neq 0, \delta \neq 0] \ \equiv \ H_{lvs}\colon\ [\theta \neq 0, \vartheta' \neq 1, \delta' \neq 1].$$

Figure 1. An Illustration of seven types of shifts in a standard (exponentiated) normal distribution

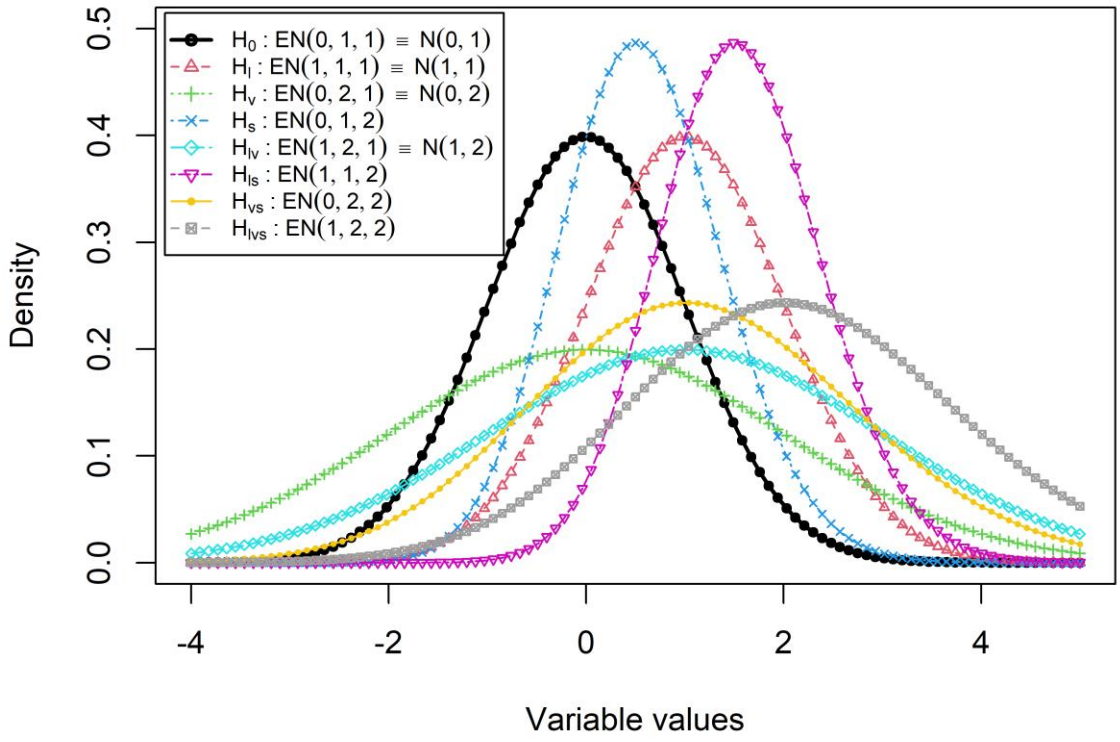

Figure 1 explains seven types of shifts in the standard (exponentiated) normal distribution. While alternatives of the types H_l, H_v, H_s or H_{lv} are addressed in literature more frequently, other possibilities are not well-addressed. Kössler & Mukherjee (2020) proposed a two-sample test that is powerful for all possible alternatives involving the three parameters. Their idea was to modify the Lepage statistic, that is sensitive to location and/or scale shifts, to be sensitive also to shape shifts. More precisely, writing $S = \frac{SA-\mu_{SA}}{\sigma_{SA}}$, they considered the Euclidean distance of $\left(\frac{WI-\mu_{WI}}{\sigma_{WI}}, \frac{AB-\mu_{AB}}{\sigma_{AB}}, \frac{SA-\mu_{SA}}{\sigma_{SA}}\right) = (L, V, S)$ from (0,0,0) as

$$T = \left(\frac{W-\mu_W}{\sigma_W}\right)^2 + \left(\frac{AB-\mu_{AB}}{\sigma_{AB}}\right)^2 + \left(\frac{SA-\mu_S}{\sigma_S}\right)^2 = L^2 + V^2 + S^2.$$

Note that, L, V and S being standardized, $E(L|IC) = E(V|IC) = E(S|IC) = 0$, and $Var(L|IC) = Var(V|IC) = Var(S|IC) = 1$. Therefore, we always have $E(T|IC) = E(L^2 + V^2 + S^2|IC) = 3$. Irrespective of the magnitude, nature and direction of the possible shifts in location, scale and shape, one may expect in most situations, $E(T|OOC) > 3$. Kössler, & Mukherjee (2020) referred to the statistic T as the $ECWAS$ statistic. In the context of process

monitoring, we propose a comprehensive tri-aspect Phase-II monitoring scheme for versatile shifts can be designed based on the $ECWAS$ statistic, referred to as the LVS scheme, for joint surveillance of location, variability and shape, and we discuss its implementation in the next section.

3. Implementation of the LVS chart

The LVS distribution-free chart for versatile shifts is a comprehensive, integrated scheme that ensures monitoring location, scale and shape aspects. The charting scheme plots the location (L), variability (V) and shape (S) components as standardized Wilcox, AB and Savage-type statistics, as well as their sum of squares (T) as the plotting statistic for the overall assessment of the process in the Y-axis against the sample number in X-axis. Since $T \geq 0$, $y_{axis} = 0$ may be treated as the baseline for the overall assessment; and further $E(L|IC) = E(V|IC) = E(S|IC) = 0$; so baseline also serves as the central line of the component sub-charts. As noted earlier, $E(T|IC) = 3$. Therefore, $y_{axis} = 3$ can serve as the central line for the overall assessment. Also, under IC, L, V and S are approximately distributed as standard normal, so, $y_{axis} = 3$ serves as the upper 3σ-control limit of the component sub-charts, and we consider $y_{axis} = -3$ as the lower 3σ control limit of the component sub-charts. For overall assessment, T is compared with the upper control limit (UCL), say H, and a median line (ML) may be considered to see any presence of runs in T. Here ML is such that $P(T > ML|IC) = 0.5$. Determination of the ML and H is deferred to Section 3.3.

3.1. Implementation steps for the LVS chart

Step 1: Perform Phase-I analysis. More precisely, collect a random reference sample $\boldsymbol{X_m} = \{X_1, \dots, X_m\}$ of size m from an IC process after a suitable Phase-I analysis, like the RS/P procedure by Capizzi,& Masarotto (2013) or that by Li, Mukherjee,& Su (2019). The previous methods can establish whether the reference sample is compatible with a stable process concerning the location and scale aspect. No method for all three parameters is available yet.

Step 2: In the course of Phase-II monitoring, observe the j^{th} test-sample ($j = 1, 2, \dots$) of size n as $\boldsymbol{Y_{j,n}} = \{Y_{j1}, \dots, Y_{jn}\}$ at the j^{th} stage of inspection.

Step 3: Compute the component plotting statistics L, V, S and the statistic T of the LVS scheme to compare the j^{th} test-sample ($j = 1, 2, \ldots$) with the reference sample and denote them by $L_j, V_j, S_j,$ and T_j.

Step 4: Plot T_j against the specified upper control limit (UCL), say H. The central line (CL) is $CL = E(T_j|IC) = 3$. When the process is *OOC*, irrespective of the number, nature and direction of possible shifts in location, scale and shape, it is $E(T_j|OOC) > 3$ and therefore there is only the upper control limit (UCL). Also, plot L_j, V_j and S_j for the sub-charts for the location, scale and shape components respectively. While T_j of the main chart may be indicated by a small circle, L_j, V_j and S_j maybe marked by L, V and S for easy identification of the component that they represent.

Step 5: If $T_j > H$, we suspect a possible shift in the process at the j^{th} step and the search for an assignable cause begins.

Step 6: Post-signal Follow-up Procedure. We check if L, V and S are greater than +3 or less than -3 and accordingly conclude whether there is a change in either the location or scale or shape or in more than one of the three parameters. A run of L or V or S above or below the baseline (that is the central line of the component charts), also indicate a possible shift in the corresponding parameter. Two situations may not be ruled out. First, a signal in the LVS chart but not signal in either of the component charts and second, a signal in one of the component charts but not in the LVS chart. In the first case, one can easily find the dominant components amongst $|L|$, $|V|$ and $|S|$ and consider it as a primary cause of the signal. In the second situation, it will be advisable to inspect if there is any run, otherwise, continue sampling.

It is important to emphasize that the post signal follow-up for the comprehensive LVS scheme is straightforward compared to any other existing schemes and fully integrated. This is a significant practical advantage of the proposed scheme.

3.2. Determination of Median Line and Upper Control Limit

We now discuss the search algorithm for *H*. To this end, note the following result.

Result 1. For a sequence of independently identically distributed reference sample of size m and test sample of size n, as $\min\{m, n\} \to \infty$, the limiting IC distribution of $T_j, \forall\, j$, is approximately

equivalent to the distribution of $1.73Z + 0.27$, where Z follows a χ^2 distribution with 1.579 degrees of freedom (df).

Proof. See Kössler & Mukherjee (2020).

Result 2. (i) Conditionally on $\boldsymbol{X_m}$, the distribution of the run-length variable R_T of the LVS scheme is geometric, and is given by,

$$P[R_T = t|\boldsymbol{X_m}, IC] = P[T_1 < H|\boldsymbol{X_m}, IC]^{t-1}(1 - P[T_1 < H|\boldsymbol{X_m}, IC]).$$

(ii) Conditional *IC* Average Run-length ($CARL_0$) given $\boldsymbol{X_m}$, is given by

$$E(R_T|\boldsymbol{X_m}, IC) = \frac{1}{1 - P[T_1 < H|\boldsymbol{X_m}, IC]}.$$

(iii) (Unconditional) *IC* Average Run-length (ARL_0) is given by

$$E(R_T|IC) = E\left[\frac{1}{1 - P[T_1 < H|\boldsymbol{X_m}, IC]}\right].$$

Proof. Note that, given $\boldsymbol{X_m}$ T_j's are independent as each T_j depends only on the j^{th} test sample, and consequently, outcomes with successive test samples become a sequence of Bernoulli trials with success being the probability of boundary-crossing, that is,

$$P[T_1 \geq H|\boldsymbol{X_m}, IC] = 1 - P[T_1 < H|\boldsymbol{X_m}, IC].$$

The result (i) follows from the probability of first boundary crossing at the t^{th} trial. Result (ii) follows from the properties of Geometric distribution defined over the set of natural numbers as its support. Finally, (iii) follows integrating $E(R_T|\boldsymbol{X_m}, IC]$ over the range of $\boldsymbol{X_m}$.

As a consequence of Result 2(iii), using Jensen's inequality, we find that

$$E(R_T|IC) = E\left[\frac{1}{1 - P[T_1 < H|\boldsymbol{X_m}, IC]}\right] \geq \frac{1}{1 - E\left[P[T_1 < H|\boldsymbol{X_m}, IC]\right]} = \frac{1}{1 - P[T_1 < H|\, IC]}.$$

Also from Result 1, one may approximate

$$\frac{1}{\tau} \leq\ P[T_1 \geq H|\, IC] = P\left[Z \geq \frac{H - 0.27}{1.73}|IC\right]\ \text{ or }\ P\left[Z < \frac{H - 0.27}{1.73}|IC\right] \leq 1 - \frac{1}{\tau}.$$

Therefore, given the target ARL_0, say τ, one may choose the starting value of H, say $H_{start} = 0.27 + 1.73\chi^2_{1-\frac{1}{\tau},1.579}$, where $\chi^2_{\xi,1.579}$ is the upper 100ξ percent point of the the χ^2 distribution with 1.579 df. Note that, the approximation is far from being accurate in the tail region, especially with small samples. In this paper, we use Monte-Carlo simulation in determining control limits

and for performance analysis because the test sample size is almost always very small in the context of Phase-II monitoring. The large sample results are used to find starting values of Monte-Carlo simulation for determination of control limits. Therefore, following search algorithm has been developed to improved estimation of H. Let ∇ be a reasonably small positive value.

Search Algorithm

1. Set $H_{trail} = H_{start}$
2. Compute the ARL_0 at H_{trail}, say ARL_{0trail}, and record $(ARL_{0trail}, H_{trail})$
3. If $ARL_{0trail} < \tau$; set $H_{trail} = H_{trial} + \nabla$, else if $ARL_{0trail} > \tau$; set $H_{trail} = H_{trial} - \nabla$,
4. Repeat step 2 and 3 until $ARL_{0trail} - \tau$ changes its sign
5. Fit a locally weighted regression $H = f(ARL_{0trail})$ based on all $(ARL_{0trail}, H_{trail})$ pairs
6. Predict $UCL = H$ from the fitted model in Step-5

It is worth noting that the convergence as in Result 1 is reasonably accurate towards the central part of the distribution and therefore it is safe to consider $0.27 + 1.73\chi^2_{0.5,1.579} = 1.97$ as the median line ML. However, it can also be more precisely estimated via simulation.

4. Performance comparison study

In this section, we first study the ICrobustness of the LVS scheme. More precisely, we compute the ARL_0 using Monte-Carlo simulation for different process distributions for a given (m, n, H) to verify the distribution-free characteristics of the proposed scheme. Further, we compare the OOC-ARL values of the proposed scheme with the Shewhart-Lepage (SL) scheme as in Mukherjee,& Chakraborti (2012), the Shewhart-Cucconi (SC) scheme as in Chowdhury, Mukherjee, & Chakraborti (2014), and the adaptive $MLPA$ scheme, as in Song, Mukherjee, Liu, & Zhang (2019) for location-scale shifts. Both SL and SC schemes are well established nonparametric schemes for detecting joint shifts in location and scale, whereas the $MLPA$ scheme is a more recent addition to the literature of location-scale schemes. The SL scheme is based on two components of the proposed chart. The $MLPA$ scheme is an adaptive scheme based on Lepage-type statistics. It is meaningful to compare the proposed scheme with these competing schemes because there is evidence that both the Lepage and Cucconi tests are sensitive also against differences in shape, see Marozzi (2013), and Song, Mukherjee, Liu, & Zhang (2019) showed that the $MLPA$ scheme can be useful also for detecting a shape shift. A recent study by Chong, Huang, Mukherjee, & Yang

(2020) also established that the SL and SC schemes are useful even for three or four-parameter processes. We study the performance of these schemes in identifying various possible shifts in location, scale and shape when the process distributions are: i) standard normal; ii) standard Laplace; iii) standard Cauchy; and iv) exponential with mean equal to 1. These distributions range from light to heavy-tailed ones and from symmetric to skewed ones, therefore covering a wide range of practical situations. More precisely, distribution (ii) is heavy-tailed and symmetric, distribution (iii) is very heavy-tailed and symmetric, distribution (iv) is skewed.

4.1. IC performance

The IC situation is simulated by setting $(\theta, \vartheta', \delta') = (0,1,1)$. The ARL, standard deviation ($SDRL$) and 5th, 25th, 50th, 75th and 95th percentiles of the run-length are computed for the various process distributions and for two popular target ARL_0 values: 370 and 500. The considered reference and test sample sizes are $(m, n) = (50,5)$, (50,10), (100,5), (100,10), (300,5), (300,10), (500,5), (500,10) that cover a wide range of possible practical situations. In this paper, 10000 replications of Monte Carlo are considered for computing ARL_0 and $SDRL_0$. Table 1 displays the performance of the proposed chart when the process is IC along with the charting parameter H. The cells corresponding to each of the four distributions contain the run-length statistics in two lines, where the first line displays the ARL_0 and $SDRL_0$ within parenthesis, and the second line shows the 5th, 25th, 50th, 75th and 95th percentiles of the run-length distribution. The IC results are consistent with the distribution-freeness of the LVS chart because the estimated ARL_0 values are very close to the target values irrespective to the distribution of the process. Percentile values show that the run length distribution of the proposed chart is highly-right-skewed because for example the ARL_0 is much larger than the median and the 95th percentile is generally several times higher than the ARL_0. Right-skewness of the run-length distribution is not surprising and has been found by many other authors, see for example Zhang, Li, & Li (2017) or Song, Mukherjee, Liu, & Zhang (2019). Note that, the conditional run length distribution being geometric with probability $P[T_1 > H|\boldsymbol{X_m}, IC]$,

$$Var(R_T|IC) = Var[E(R_T|\boldsymbol{X_m}, IC)] + E[Var(R_T|\boldsymbol{X_m}, IC)]$$

For conditional run-length distribution, $E(R_T|\boldsymbol{X_m}, IC) \approx SD(R_T|\boldsymbol{X_m}, IC)$, $P[T_1 > H|\boldsymbol{X_m}, IC]$ being a small positive proper fraction. But owing to the component, $Var[E(R_T|\boldsymbol{X_m}, IC)]$, we observe in Table 1 that unconditionally, $SDRL_0$ values are higher than the ARL_0.

Table 2: Upper Control limit (H) and IC robustness of the proposed chart for selected (m, n) and Target $ARL_0 = 370$, and 500

Target $ARL_0 = 370$						
m	n	H	Normal	Laplace	Cauchy	Exponential
50	5	15.89	370.98 (669.31) 8, 48, 141, 384, 496	371.27 (662.85) 7, 48, 141, 388, 1512	372.85 (678.61) 7, 47, 142, 386, 1529	378.35 (676.16) 7, 48, 145, 394, 1529
	10	14.60	371.14 (661.66) 7, 44, 136, 389, 1559	375.73 (681.52) 7, 44, 138, 379, 1623	375.32 (672.53) 7, 44, 139, 396, 1589	376.88 (672.49) 7, 45, 140, 399, 1526
100	5	17.92	364.90 (572.91) 11, 62, 169, 421, 1394	368.65 (579.62) 11, 62, 170, 424, 1376	364.30 (563.20) 10, 61, 171, 426, 1359	370.29 (579.38) 11, 63, 174, 429, 1364
	10	16.49	377.18 (601.41) 10, 58, 166, 430, 1467	368.17 (582.13) 9, 58, 167, 428, 1370	373.93 (586.51) 10, 60, 170, 427, 1422	364.60 (571.40) 10, 59, 166, 418, 1417
300	5	20.35	371.26 (479.23) 15, 82, 211, 468, 1268	375.40 (485.29) 15, 86, 216, 471, 1258	370.79 (470.17) 15, 86, 216, 474, 1239	370.92 (478.5) 15, 84, 211, 469, 1269
	10	18.75	368.19 (480.63) 13, 79, 206, 462, 1263	369.64 (480.63) 14, 80, 206, 472, 1253	365.54 (487.18) 14, 79, 205, 453, 1251	370.32 (485.18) 14, 81, 209, 464, 1277
500	5	21.03	370.93 (451.08) 16, 88, 225, 486, 1218	369.41 (440.87) 16, 90, 226, 484, 1202	366.48 (428.17) 16, 92, 227, 483, 1182	371.34 (446.82) 16, 89, 226, 483, 1223
	10	19.47	372.74 (463.60) 16, 88, 222, 477, 1242	370.08 (457.94) 15, 85, 220, 478, 1244	376.53 (468.90) 16, 86, 222, 482, 1252	376.12 (462.01) 16, 89, 223, 488, 1251
Target $ARL_0 = 500$						
m	n	H	Normal	Laplace	Cauchy	Exponential
50	5	16.90	508.78 (860.82) 10, 63, 191, 543, 2157	501.64 (847.33) 9, 62, 194, 534, 2090	503.33 (856.34) 10, 61, 186, 525, 2203	500.67 (845.97) 10, 63, 193, 525, 2145
	10	15.33	495.67 (858.64) 9, 55, 176, 518, 2194	497.21 (844.38) 8, 57, 182, 534, 2155	491.35 (847.74) 8, 58, 182, 514, 2108	500.03 (851.50) 9, 57, 181, 531, 2162
100	5	19.13	497.14 (744.95) 13, 81, 231, 583, 1886	498.45 (750.61) 14, 82, 232, 573, 1962	498.45 (750.61) 14, 82, 232, 573, 1962	499.82 (774.52) 14, 80, 223, 563, 1995
	10	17.42	505.23 (785.29) 13, 75, 223, 567, 2041	497.71 (767.71) 12, 75, 217, 573, 1982	501.19 (781.07) 12, 74, 217, 570, 2018	499.58 (780.55) 12. 76, 219, 568, 1988
300	5	21.72	504.49 (638.30) 20, 111, 286, 641, 1755	492.20 (644.84) 19, 106, 275, 616, 1703	503.80 (651.46) 19, 108, 282, 637, 1762	499.11 (647.04) 19, 111, 282, 626, 1707
	10	19.95	494.21 (651.42) 18, 102, 273, 622, 1694	500.78 (659.23) 18, 103, 274, 631, 1766	491.93 (648.54) 18, 103, 272, 619, 1703	501.34 (648.55) 18, 104, 277, 629, 1767
500	5	22.60	500.49 (598.44) 21, 120, 299, 660, 1663	499.24 (595.21) 22, 121, 304, 650, 1639	494.17 (595.64) 20, 118, 298, 643, 1625	501.14 (605.55) 21, 120, 303, 654, 1652
	10	20.74	502.18 (614.41) 20, 116, 296, 644, 1689	502.97 (625.17) 20, 117, 292, 651, 1671	489.41 (598.56) 21, 114, 290, 636, 1635	501.30 (625.71) 20, 112, 294, 647, 1682

Note that, we use the $H_{start} = 18.83$ for target $ARL_0 = \tau = 370$ and $H_{start} = 19.84$ for target $ARL_0 = \tau = 500$, as indicated in Section 3.2. We observe from Table 2 that the simulated H values increase as m increases and decrease and n increases, with a fair indication that for large (m, n), H_{start} itself may be considered as an approximate upper control limit.

4.2. *OOC* performance

The results of OOC comparison study are displayed in Figure 2 and Tables 4-7. Various OOC situations are simulated by setting $\theta \neq 0$ or $\vartheta' \neq 1$ or $\delta' \neq 1$. Again, 20000 iterations of Monte Carlo are considered for computing the run-length properties for each set of $(\theta, \vartheta', \delta')$. For

brevity, we present the results for (m, n) =(100,5) and ARL_0 =500. We consider a large number of OOC situations with small to large shifts in either one, or two, or all of the location, scale and shape parameters. Figure 2 displays the OOC-ARL values of the four competing schemes when there is a shift in only one of the three parameters. First, we consider a pure location shift from $F(\theta = 0, \vartheta' = 1, \delta' = 1)$ to $F(\theta; \vartheta' = 1, \delta' = 1)$ for eight equispaced values of θ in the interval 0.25 to 2, including both the boundaries and compute the OOC-ARL values. The IC and OOC-ARL values corresponding to $\theta = 0(0.25)2$, for four distributions as before, are plotted in four panels, respectively in the 1st row of Figure 2. In the 2nd row of Figure 2, ARL comparisons under a pure scale shift are presented. Here, the plot is generated via the IC-ARL for $\vartheta' = e^{\vartheta} = 1$, and simulated OOC-ARL values corresponding to a shift in e^{ϑ}, for eight equispaced values of ϑ in the interval of 0.15 to 1.2. That is, the 2nd row displays the nine values of ϑ' in the interval 1 to 3.32 and the corresponding ARL values when the other parameters are in the IC state. Finally, the 3rd row of Figure 2 shows the performance comparisons under a pure shift in the shape parameter. To this end, the plot is generated using the IC-ARL for $\delta' = e^{\delta} = 1$, and simulated OOC-ARL values corresponding to a shift in e^{δ}, for eight equispaced values of ϑ in the interval of 0.25 to 2. That is, the 2nd row displays the nine values of δ' in the interval 1 to 7.39 and the corresponding ARL values when the other parameters are in the IC state.

Figure 2 indicates that the proposed scheme performs markedly better than the competing ones in the presence of an isolated location shift. Most of the existing joint monitoring schemes display ARL-biasedness for a small shift in location, that is, for small $\theta \in (0,0.25)$ often the OOC-ARL is found higher than the target ARL_0 . The LVS scheme does not display any ARL-biasedness. The proposed scheme performs markedly better than the other ones in the presence of a solitary scale shift when the process distribution is exponential, that is, skewed. The $MLPA$ scheme has the smallest ARL when the process distribution is symmetric, that is, for the normal, Laplace and Cauchy distributions. For symmetric distributions, the performance of the proposed scheme in detecting isolated scale shift lies in between the SL and SC schemes, making it a safer choice when process distribution is actually unknown. As expected, the proposed scheme has the smallest ARL in the presence of an isolated upward shift in the shape parameter. Note, however, that for a downward shift in the shape parameter, the $MLPA$ scheme has some advantage over the proposed LVS scheme. This is not surprising as the S component of the LVS scheme is more suitable for an

Figure 2: Comparison of $OOC\text{-}ARL$ of Various Schemes under Isolated Shift in One of the Three Process Parameters for $m = 100, n = 5$ and target $ARL_0 = 500$.

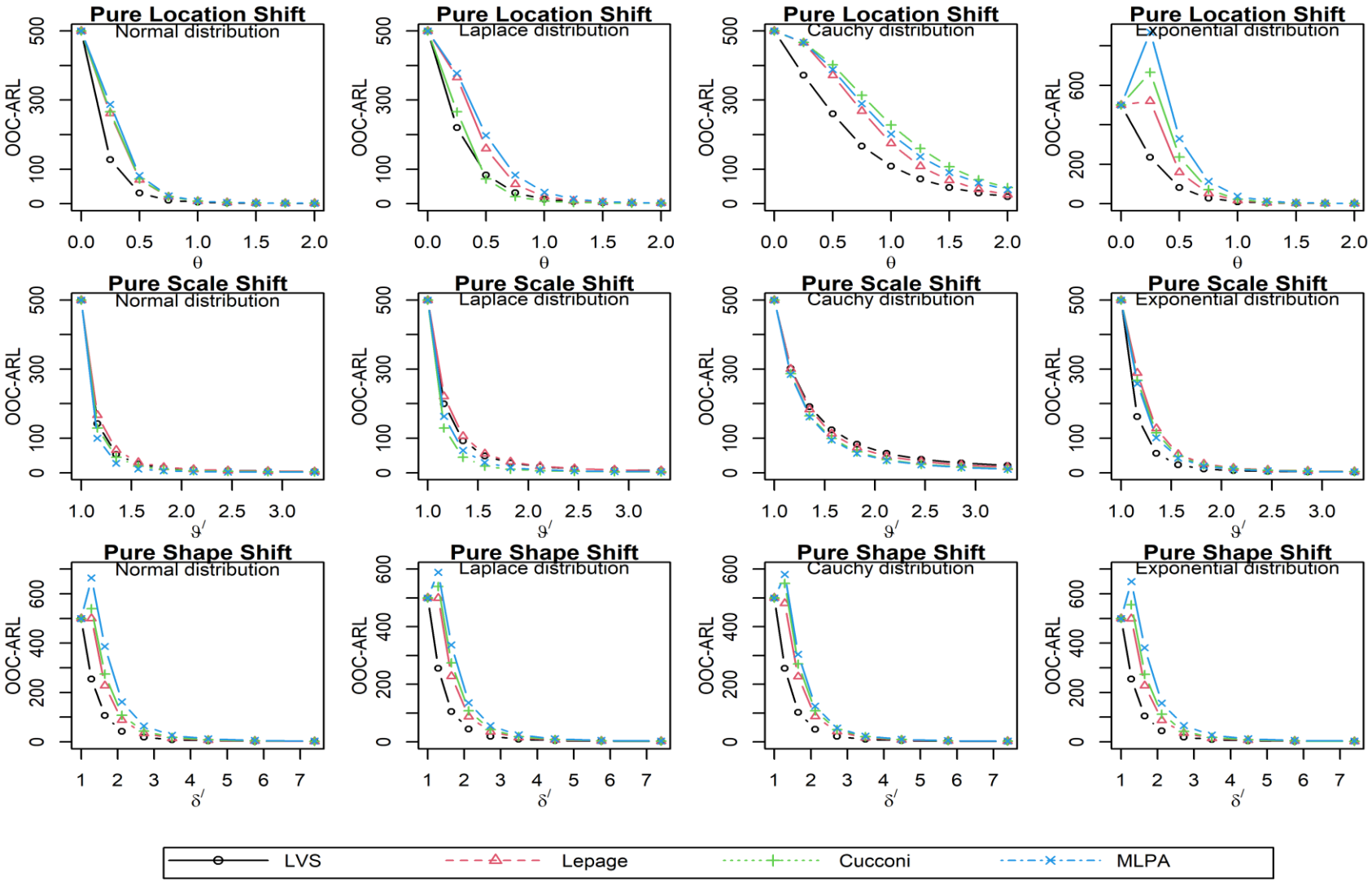

upward shift in the shape parameter. A savage-type test for downward shift also exists, future research is highly warranted for integrating it in an adaptive SPM scheme.

For assessing the chart performance under a shift in two or more parameters, we consider four values of θ as 0.5, 1, 2, 3; four values of ϑ' as 1.25, 1.5, 2, 3; and four values of δ' as 0.5, 2, 5, 10. To save space, we only present the ARL values along with corresponding $SDRL$ values in parenthesis and omit percentile values. The cells with the smallest $OOC\text{-}ARL$ values are grey-shaded, ignoring minor sampling fluctuations. Table 3 displays the ARL of the schemes when a shift occurs in both the location and scale parameters. It is observed that the proposed scheme is the preferred one having the smallest ARL for any location shift accompanied by a small scale shift. When there is a significant scale shift along with the location shift, the $MLPA$ scheme is found to be marginally superior to the proposed schemes. Even in such cases, the difference in the $OOC\text{-}ARL$ between the best scheme and the proposed scheme is negligible except for a few settings.

Table 3: Comparison of $OOC\text{-}ARL$ of Various Schemes when a Shift Occurs in both the Location and Scale Parameters for $m = 100, n = 5$ and target $ARL_0 = 500$

OOC Parameters	Proposed Scheme	SL Scheme	SC Scheme	$MLPA$ scheme
	Normal Distribution			
(0.5, 1.25, 1)	13.48 (16.27)	31.07 (40.29)	26.18 (33.59)	21.37 (28.3)
(0.5, 1.5, 1)	8.51 (9.16)	18.09 (20.28)	13.58 (15.09)	9.09 (10.13)
(0.5, 2, 1)	5.09 (4.83)	8.7 (8.51)	5.81 (5.61)	3.54 (3.24)
(0.5, 3, 1)	3.26 (2.77)	3.94 (3.5)	2.57 (2.05)	1.67 (1.09)
(1, 1.25, 1)	3.54 (3.37)	6.75 (7.12)	6.15 (6.5)	5.48 (5.93)
(1, 1.5, 1)	3.19 (2.87)	6.06 (6.09)	5.20 (5.14)	4.12 (3.99)
(1, 2, 1)	2.76 (2.3)	4.89 (4.61)	3.76 (3.36)	2.6 (2.14)
(1, 3, 1)	2.37 (1.82)	3.30 (2.81)	2.31 (1.78)	1.58 (0.99)
(2, 1.25, 1)	1.15 (0.42)	1.42 (0.8)	1.36 (0.72)	1.29 (0.64)
(2, 1.5, 1)	1.22 (0.53)	1.60 (1.02)	1.51 (0.90)	1.37 (0.74)
(2, 2, 1)	1.34 (0.68)	1.90 (1.34)	1.71 (1.13)	1.45 (0.83)
(2, 3, 1)	1.49 (0.86)	2.08 (1.52)	1.70 (1.10)	1.33 (0.68)
	Laplace Distribution			
(0.5, 1.25, 1)	34.03 (53.93)	66.08 (100.35)	60.12 (94.22)	56.68 (97.61)
(0.5, 1.5, 1)	19.50 (26.73)	36.14 (46.54)	28.76 (37.83)	24.37 (32.88)
(0.5, 2, 1)	9.99 (11.19)	16.44 (18.26)	11.33 (12.46)	8.67 (10.05)
(0.5, 3, 1)	5.27 (5.11)	6.66 (6.47)	4.30 (4.01)	3.24 (3.05)
(1, 1.25, 1)	8.48 (11.68)	14.23 (22.15)	15.10 (25.30)	16.2 (27.89)
(1, 1.5, 1)	6.61 (7.95)	11.15 (13.76)	10.44 (13.60)	10.02 (12.93)
(1, 2, 1)	4.87 (5.02)	7.94 (8.74)	6.32 (6.81)	5.37 (5.78)
(1, 3, 1)	3.51 (3.17)	4.86 (4.60)	3.39 (3.03)	2.68 (2.34)
(2, 1.25, 1)	1.63 (1.17)	2.00 (1.61)	1.99 (1.70)	2.19 (2.16)
(2, 1.5, 1)	1.70 (1.22)	2.15 (1.74)	2.06 (1.70)	2.18 (1.90)
(2, 2, 1)	1.78 (1.28)	2.35 (1.9)	2.13 (1.71)	2.06 (1.66)
(2, 3, 1)	1.84 (1.28)	2.43 (1.95)	1.97 (1.46)	1.75 (1.23)

	Cauchy Distribution			
(0.5, 1.25, 1)	139.16 (272.74)	183.64 (294.58)	180.72 (301.96)	178.41 (326.89)
(0.5, 1.5, 1)	88.00 (160.88)	107.51 (161.26)	99.15 (162.06)	94.74 (156.41)
(0.5, 2, 1)	43.94 (69.98)	48.13 (65.03)	41.34 (62.63)	38.23 (56.85)
(0.5, 3, 1)	19.68 (26.85)	18.91 (22.72)	13.85 (18.3)	12.58 (16.2)
(1, 1.25, 1)	68.04 (164.49)	99.94 (215.64)	115.21 (252.23)	104.77 (229.85)
(1, 1.5, 1)	47.13 (102.06)	61.79 (111.83)	67.08 (122.14)	61.78 (120.3)
(1, 2, 1)	27.45 (49.89)	32.98 (48.64)	30.96 (52.39)	28.22 (44.37)
(1, 3, 1)	14.62 (20.54)	15.64 (19.99)	12.03 (16.23)	11.01 (14.86)
(2, 1.25, 1)	14.99 (38.8)	18.71 (76.08)	29.12 (105.36)	25.57 (91.6)
(2, 1.5, 1)	12.70 (32.55)	14.90 (37.12)	20.65 (58.37)	18.42 (50.47)
(2, 2, 1)	10.03 (18.71)	11.53 (22.35)	13.15 (28.32)	12.04 (25.69)
(2, 3, 1)	7.57 (10.92)	8.53 (11.01)	7.42 (10.73)	6.76 (9.18)
	Exponential Distribution			
(0.5, 1.25, 1)	18.94 (30.7)	43.4 (72.97)	48.36 (87.93)	59.27 (145.8)
(0.5, 1.5, 1)	8.1 (10.55)	17.79 (24.06)	18.49 (26.74)	19.4 (30.52)
(0.5, 2, 1)	3.26 (3.16)	6.41 (7.16)	6.13 (6.82)	5.88 (6.92)
(0.5, 3, 1)	1.63 (1.07)	2.6 (2.19)	2.47 (2.08)	2.21 (1.79)
(1, 1.25, 1)	4.06 (6.05)	6.56 (10.18)	7.94 (13.14)	10.41 (18.23)
(1, 1.5, 1)	2.52 (2.65)	3.79 (4.75)	4.29 (5.49)	5.06 (7.17)
(1, 2, 1)	1.58 (1.10)	2.15 (1.97)	2.28 (2.07)	2.43 (2.37)
(1, 3, 1)	1.16 (0.46)	1.40 (0.83)	1.41 (0.84)	1.40 (0.82)
(2, 1.25, 1)	1.04 (0.24)	1.03 (0.21)	1.07 (0.39)	1.23 (0.81)
(2, 1.5, 1)	1.02 (0.17)	1.01 (0.15)	1.04 (0.25)	1.13 (0.50)
(2, 2, 1)	1.01 (0.09)	1.01 (0.09)	1.01 (0.14)	1.05 (0.26)
(2, 3, 1)	1.00 (0.04)	1.00 (0.04)	1.00 (0.06)	1.01 (0.12)

Table 4 displays the ARL of the schemes when a shift occurs in both the scale and shape parameters. Table 4 shows that the proposed scheme performs markedly better than the other ones, except when the downward shift in the shape parameter is present, where the $MLPA$ has smaller ARL. Note that no distribution-free charting scheme for a mixed shift involving scale and shape parameters is discussed in the current literature to the best of our knowledge.

Table 4: Comparison of OOC-ARL of Various Schemes when a Shift Occurs in both the Scale and Shape Parameters for $m = 100, n = 5$ and target $ARL_0 = 500$

OOC Parameters	Proposed Scheme	SL Scheme	SC Scheme	$MLPA$ scheme
	Normal Distribution			
(0, 1.25, 0.5)	23.28 (25.38)	7.94 (7.99)	6.56 (6.66)	4.92 (4.96)
(0, 1.25, 2)	11.27 (14.44)	24.67 (32.93)	24.41 (34.29)	25.32 (39.66)
(0, 1.25, 5)	1.60 (1.12)	2.14 (1.82)	2.19 (1.93)	2.37 (2.33)
(0, 1.25, 10)	1.03 (0.20)	1.07 (0.29)	1.08 (0.31)	1.11 (0.4)
(0, 1.5, 0.5)	14.69 (15.02)	5.16 (4.91)	4.08 (3.73)	2.92 (2.51)
(0, 1.5, 2)	5.32 (5.64)	11.21 (12.78)	10.1 (11.5)	8.87 (10.35)
(0, 1.5, 5)	1.23 (0.56)	1.54 (0.99)	1.51 (0.95)	1.50 (0.95)
(0, 1.5, 10)	1.01 (0.07)	1.02 (0.14)	1.02 (0.14)	1.02 (0.14)
(0, 2, 0.5)	8.85 (8.50)	3.16 (2.68)	2.43 (1.89)	1.75 (1.17)
(0, 2, 2)	2.66 (2.24)	4.98 (4.74)	4.18 (3.92)	3.23 (2.90)
(0, 2, 5)	1.06 (0.25)	1.21 (0.52)	1.18 (0.47)	1.13 (0.40)
(0, 2, 10)	1.00 (0.02)	1.00 (0.06)	1.00 (0.05)	1.00 (0.04)

	Laplace Distribution			
(0, 1.25, 0.5)	28.33 (31.98)	9.45 (10.05)	7.98 (8.27)	7.23 (8.04)
(0, 1.25, 2)	16.14 (22.84)	35.11 (53.16)	36.47 (58.81)	41.30 (73.84)
(0, 1.25, 5)	1.88 (1.59)	2.51 (2.42)	2.69 (2.79)	2.96 (3.49)
(0, 1.25, 10)	1.06 (0.28)	1.11 (0.38)	1.13 (0.43)	1.17 (0.56)
(0, 1.5, 0.5)	18.81 (20.04)	6.56 (6.5)	5.3 (5.15)	4.68 (4.70)
(0, 1.5, 2)	8.4 (10.47)	17.29 (22.01)	16.63 (21.88)	17.45 (23.91)
(0, 1.5, 5)	1.41 (0.87)	1.80 (1.35)	1.84 (1.44)	1.93 (1.59)
(0, 1.5, 10)	1.02 (0.14)	1.04 (0.21)	1.04 (0.22)	1.06 (0.26)
(0, 2, 0.5)	11.71 (11.72)	4.14 (3.76)	3.25 (2.83)	2.76 (2.45)
(0, 2, 2)	4.04 (3.94)	7.66 (8.16)	6.83 (7.27)	6.54 (7.22)
(0, 2, 5)	1.14 (0.42)	1.35 (0.73)	1.33 (0.71)	1.34 (0.73)
(0, 2, 10)	1.00 (0.04)	1.01 (0.1)	1.01 (0.09)	1.01 (0.1)
	Cauchy Distribution			
(0, 1.25, 0.5)	35.75 (43.31)	11.80 (13.28)	10.25 (11.75)	11.27 (12.9)
(0, 1.25, 2)	27.81 (51.1)	52.24 (95.18)	62.16 (138.2)	70.58 (143.25)
(0, 1.25, 5)	2.38 (2.55)	3.07 (3.64)	3.54 (5.02)	3.78 (5.72)
(0, 1.25, 10)	1.12 (0.43)	1.16 (0.5)	1.23 (0.66)	1.24 (0.71)
(0, 1.5, 0.5)	25.93 (30.32)	8.94 (9.78)	7.76 (8.45)	8.45 (9.41)
(0, 1.5, 2)	17.24 (28.99)	30.56 (51.75)	35.18 (73.51)	39.19 (75.95)
(0, 1.5, 5)	1.87 (1.68)	2.30 (2.29)	2.54 (2.82)	2.69 (3.03)
(0, 1.5, 10)	1.06 (0.28)	1.08 (0.33)	1.11 (0.43)	1.13 (0.46)
(0, 2, 0.5)	16.97 (18.55)	6.07 (6.23)	5.12 (5.25)	5.38 (5.48)
(0, 2, 2)	9.09 (13.16)	14.46 (20.74)	15.77 (24.72)	17.67 (29.51)
(0, 2, 5)	1.42 (0.92)	1.65 (1.22)	1.74 (1.48)	1.82 (1.55)
(0, 2, 10)	1.02 (0.14)	1.03 (0.18)	1.04 (0.22)	1.05 (0.25)
	Exponential Distribution			
(0, 1.25, 0.5)	76.07 (91.02)	23.84 (28.51)	19.65 (23.37)	15.28 (19.14)
(0, 1.25, 2)	10.22 (13.96)	20.36 (29.36)	22.14 (34.15)	26.46 (49.53)
(0, 1.25, 5)	1.51 (1.05)	1.86 (1.53)	1.99 (1.8)	2.32 (2.41)
(0, 1.25, 10)	1.03 (0.19)	1.05 (0.24)	1.06 (0.28)	1.11 (0.42)
(0, 1.5, 0.5)	76.33 (87.97)	30.16 (35.57)	23.05 (27.36)	15.86 (19.44)
(0, 1.5, 2)	4.20 (4.58)	7.73 (9.31)	7.72 (9.66)	8.28 (11.21)
(0, 1.5, 5)	1.15 (0.45)	1.29 (0.67)	1.31 (0.7)	1.38 (0.85)
(0, 1.5, 10)	1.00 (0.05)	1.01 (0.08)	1.01 (0.09)	1.02 (0.14)
(0, 2, 0.5)	40.16 (47.05)	33.43 (37.87)	22.1 (24.88)	13.3 (15.57)
(0, 2, 2)	1.82 (1.34)	2.80 (2.53)	2.72 (2.45)	2.65 (2.44)
(0, 2, 5)	1.01 (0.12)	1.05 (0.23)	1.04 (0.22)	1.05 (0.23)
(0, 2, 10)	1.00 (0.01)	1.00 (0.01)	1.00 (0.01)	1.00 (0.02)

Table 5 displays the ARL of the schemes when a shift occurs in both location and shape parameters. It is shown that the proposed scheme has a markedly smaller ARL than those of the other ones, except for very few settings where the $MLPA$ scheme has an ARL slightly smaller than that of the proposed scheme. In particular, the proposed schemes loses to the $MLPA$ schemes when there are small location shift in symmetric densities accompanied by a downward shift in the shape parameters. For a skewed population or for an upward shift in the shape parameters accompanied by a location shift in symmetric populations, the proposed scheme is substantially superior.

Table 5: Comparison of $OOC\text{-}ARL$ of Various Schemes when a Shift Occurs in both Location and Shape Parameters for $m = 100, n = 5$ and target $ARL_0 = 500$

OOC Parameters	Proposed Scheme	SL Scheme	SC Scheme	$MLPA$ scheme
	Normal Distribution			
(0.5, 1, 0.5)	151.88 (193.12)	80.59 (101.36)	61.13 (77.96)	44.62 (62.17)
(0.5, 1, 2)	4.23 (4.89)	6.91 (8.89)	7.59 (10.56)	9.22 (15.32)
(0.5, 1, 5)	1.14 (0.45)	1.24 (0.63)	1.29 (0.74)	1.43 (1.01)
(0.5, 1, 10)	1.00 (0.06)	1.01 (0.07)	1.01 (0.09)	1.02 (0.16)
(1, 1, 0.5)	28.46 (39.27)	58.3 (75.87)	45.95 (60.39)	35.67 (51.9)
(1, 1, 2)	1.35 (0.77)	1.7 (1.23)	1.72 (1.29)	1.81 (1.49)
(1, 1, 5)	1.00 (0.06)	1.01 (0.08)	1.01 (0.09)	1.01 (0.13)
(1, 1, 10)	1.00 (0.00)	1.00 (0.00)	1.00 (0.00)	1.00 (0.01)
(2, 1, 0.5)	2.04 (1.57)	3.35 (3.06)	3.13 (2.84)	2.84 (2.6)
(2, 1, 2)	1.00 (0.02)	1.00 (0.06)	1.00 (0.06)	1.00 (0.06)
(2, 1, 5)	1.00 (0.00)	1.00 (0.00)	1.00 (0.00)	1.00 (0.00)
(2, 1, 10)	1.00 (0.00)	1.00 (0.00)	1.00 (0.00)	1.00 (0.00)
	Laplace Distribution			
(0.5, 1, 0.5)	129.85 (155.51)	42.56 (50.06)	33.17 (39.88)	29.1 (37.86)
(0.5, 1, 2)	8.68 (15.28)	13.84 (25.49)	17.57 (35.11)	24.18 (71.54)
(0.5, 1, 5)	1.43 (1.10)	1.57 (1.29)	1.77 (1.75)	2.09 (2.54)
(0.5, 1, 10)	1.03 (0.18)	1.03 (0.19)	1.05 (0.26)	1.09 (0.41)
(1, 1, 0.5)	88.19 (132.27)	58.54 (70.49)	43.85 (54.32)	35.23 (48.52)
(1, 1, 2)	2.31 (2.66)	2.81 (3.98)	3.39 (5.06)	4.39 (8.8)
(1, 1, 5)	1.05 (0.26)	1.05 (0.26)	1.09 (0.4)	1.16 (0.64)
(1, 1, 10)	1.00 (0.04)	1.00 (0.02)	1.00 (0.05)	1.01 (0.10)
(2, 1, 0.5)	5.98 (8.37)	7.40 (9.61)	6.99 (10.05)	7.31 (11.14)
(2, 1, 2)	1.03 (0.19)	1.04 (0.23)	1.05 (0.25)	1.09 (0.43)
(2, 1, 5)	1.00 (0.00)	1.00 (0.01)	1.00 (0.01)	1.00 (0.03)
(2, 1, 10)	1.00 (0.00)	1.00 (0.00)	1.00 (0.00)	1.00 (0.00)
	Cauchy Distribution			
(0.5, 1, 0.5)	85.67 (98.63)	24.74 (28.22)	20.77 (23.92)	23.66 (27.73)
(0.5, 1, 2)	23.85 (52.19)	43.01 (117.68)	58.47 (150.27)	63.98 (208.37)
(0.5, 1, 5)	2.27 (2.83)	2.7 (3.85)	3.38 (5.41)	3.51 (6.26)
(0.5, 1, 10)	1.12 (0.45)	1.13 (0.51)	1.22 (0.74)	1.22 (0.8)
(1, 1, 0.5)	110.58 (124.47)	31.57 (35.64)	25.01 (28.3)	27.69 (32.5)
(1, 1, 2)	11.04 (23.59)	16.72 (59.38)	24.88 (73.32)	26.55 (103.25)
(1, 1, 5)	1.61 (1.62)	1.67 (1.99)	2.10 (3.14)	2.13 (3.49)
(1, 1, 10)	1.06 (0.31)	1.05 (0.27)	1.10 (0.46)	1.10 (0.54)
(2, 1, 0.5)	85.28 (126.02)	29.89 (35.69)	22.96 (28.14)	22.42 (30.24)
(2, 1, 2)	3.11 (6.08)	3.27 (10.04)	5.26 (21.86)	5.64 (26.45)
(2, 1, 5)	1.14 (0.68)	1.10 (0.62)	1.23 (1.29)	1.27 (2.00)
(2, 1, 10)	1.01 (0.14)	1.01 (0.10)	1.02 (0.19)	1.03 (0.26)
	Exponential Distribution			
(0.5, 1, 0.5)	1069.1 (2183.39)	1199.61 (2366.59)	3487.67 (4967.29)	4152.6 (5672.05)
(0.5, 1, 2)	8.4 (14.32)	13.69 (24.19)	17.57 (35.49)	26.88 (65.4)
(0.5, 1, 5)	1.42 (1.04)	1.56 (1.39)	1.75 (1.65)	2.36 (3.04)
(0.5, 1, 10)	1.03 (0.19)	1.03 (0.18)	1.05 (0.26)	1.13 (0.54)
(1, 1, 0.5)	84.26 (260.51)	202.58 (522.34)	297.37 (838.99)	469.33 (1349.12)
(1, 1, 2)	2.13 (2.49)	2.5 (3.28)	3.14 (4.92)	4.84 (11.26)
(1, 1, 5)	1.04 (0.25)	1.04 (0.25)	1.08 (0.37)	1.21 (0.74)
(1, 1, 10)	1.00 (0.04)	1.00 (0.02)	1.00 (0.05)	1.01 (0.13)
(2, 1, 0.5)	1.53 (1.85)	1.47 (2.35)	2.05 (4.82)	4.11 (11.6)
(2, 1, 2)	1.01 (0.09)	1.00 (0.07)	1.01 (0.12)	1.06 (0.39)
(2, 1, 5)	1.00 (0.00)	1.00 (0.00)	1.00 (0.01)	1.00 (0.04)
(2, 1, 10)	1.00 (0.00)	1.00 (0.00)	1.00 (0.00)	1.00 (0.00)

Table 6 displays the ARL of the schemes when a shift occurs in all three parameters. Table 6 shows that the proposed scheme is preferred when the process distribution is exponential. The proposed scheme performs very well also when the process distribution is normal, Laplace and Cauchy except for the OOC situations where the downward shift in the shape parameter is present, where the $MLPA$ has a smaller ARL.

Table 6: Comparison of OOC-ARL of Various Schemes when a Shift Occurs in All Three Parameters Simultaneously for $m = 100, n = 5$ and target $ARL_0 = 500$

OOC Parameters	Proposed Scheme	SL Scheme	SC Scheme	$MLPA$ scheme
	Normal Distribution			
(0.5, 1.25, 0.5)	46.95 (52.37)	21.64 (23.93)	15.04 (16.32)	9.48 (10.51)
(0.5, 1.25, 2)	2.58 (2.31)	4.36 (4.47)	4.25 (4.45)	4.25 (4.75)
(0.5, 1.25, 5)	1.05 (0.24)	1.12 (0.37)	1.12 (0.4)	1.14 (0.44)
(0.5, 1.5, 0.5)	23.71 (24.74)	10.12 (10.28)	6.88 (6.85)	4.27 (4.04)
(0.5, 1.5, 2)	2.02 (1.54)	3.33 (3.04)	3.15 (2.86)	2.85 (2.58)
(0.5, 1.5, 5)	1.02 (0.15)	1.08 (0.3)	1.07 (0.29)	1.06 (0.27)
(0.5, 2, 0.5)	11.01 (10.72)	4.51 (4.08)	3.13 (2.63)	2.04 (1.51)
(0.5, 2, 2)	1.60 (1.01)	2.50 (2.02)	2.26 (1.75)	1.91 (1.38)
(0.5, 2, 5)	1.01 (0.09)	1.04 (0.22)	1.03 (0.19)	1.02 (0.15)
(1, 1.25, 0.5)	19.13 (22.49)	28.52 (31.82)	18.48 (20.87)	10.88 (12.3)
(1, 1.25, 2)	1.27 (0.63)	1.65 (1.11)	1.62 (1.08)	1.57 (1.04)
(1, 1.25, 5)	1.00 (0.03)	1.01 (0.08)	1.01 (0.08)	1.01 (0.08)
(1, 1.5, 0.5)	13.90 (14.84)	14.5 (14.85)	8.83 (9.01)	4.99 (4.91)
(1, 1.5, 2)	1.23 (0.56)	1.62 (1.05)	1.56 (0.97)	1.46 (0.87)
(1, 1.5, 5)	1.00 (0.02)	1.01 (0.07)	1.00 (0.06)	1.00 (0.06)
(1, 2, 0.5)	9.00 (8.85)	5.85 (5.52)	3.72 (3.29)	2.24 (1.74)
(1, 2, 2)	1.20 (0.49)	1.58 (0.98)	1.49 (0.87)	1.34 (0.7)
(1, 2, 5)	1.00 (0.02)	1.01 (0.08)	1.00 (0.07)	1.00 (0.04)
(2, 1.25, 0.5)	2.52 (2.08)	4.51 (4.29)	3.85 (3.54)	3.10 (2.8)
(2, 1.25, 2)	1.00 (0.04)	1.01 (0.12)	1.01 (0.10)	1.01 (0.09)
(2, 1.25, 5)	1.00 (0.00)	1.00 (0.00)	1.00 (0.00)	1.00 (0.00)
(2, 1.5, 0.5)	2.90 (2.45)	5.21 (4.94)	4.03 (3.68)	2.83 (2.44)
(2, 1.5, 2)	1.00 (0.07)	1.03 (0.18)	1.02 (0.16)	1.01 (0.11)
(2, 1.5, 5)	1.00 (0.00)	1.00 (0.00)	1.00 (0.00)	1.00 (0.00)
(2, 2, 0.5)	3.38 (2.93)	4.9 (4.49)	3.28 (2.84)	2.08 (1.55)
(2, 2, 2)	1.01 (0.11)	1.07 (0.27)	1.05 (0.24)	1.03 (0.17)
(2, 2, 5)	1.00 (0.00)	1.00 (0.00)	1.00 (0.00)	1.00 (0.00)
	Laplace Distribution			
(0.5, 1.25, 0.5)	55.85 (61.13)	18.73 (20.41)	14.2 (15.46)	11.65 (13.60)
(0.5, 1.25, 2)	4.68 (5.66)	7.62 (10.31)	8.46 (11.91)	9.53 (15.05)
(0.5, 1.25, 5)	1.17 (0.51)	1.28 (0.7)	1.34 (0.82)	1.43 (1.01)
(0.5, 1.5, 0.5)	32.37 (33.93)	10.95 (11.26)	8.06 (8.21)	6.55 (6.97)
(0.5, 1.5, 2)	3.25 (3.30)	5.34 (6.08)	5.44 (6.46)	5.75 (7.02)
(0.5, 1.5, 5)	1.09 (0.33)	1.17 (0.5)	1.19 (0.53)	1.23 (0.59)
(0.5, 2, 0.5)	16.59 (16.73)	5.79 (5.54)	4.14 (3.8)	3.32 (3.08)
(0.5, 2, 2)	2.23 (1.82)	3.54 (3.38)	3.39 (3.26)	3.36 (3.27)
(0.5, 2, 5)	1.03 (0.19)	1.09 (0.33)	1.09 (0.32)	1.09 (0.33)
(1, 1.25, 0.5)	45.75 (57.36)	26.12 (29.24)	17.82 (20.46)	13.49 (16.23)
(1, 1.25, 2)	1.88 (1.61)	2.36 (2.3)	2.57 (2.7)	2.95 (3.45)
(1, 1.25, 5)	1.02 (0.16)	1.03 (0.18)	1.04 (0.23)	1.07 (0.32)
(1, 1.5, 0.5)	29.19 (33.63)	14.67 (15.44)	9.67 (10.3)	7.27 (7.98)
(1, 1.5, 2)	1.67 (1.22)	2.16 (1.86)	2.24 (2.06)	2.41 (2.32)

(1, 1.5, 5)	1.01 (0.10)	1.02 (0.15)	1.03 (0.17)	1.04 (0.22)
(1, 2, 0.5)	16.06 (16.98)	7.04 (6.87)	4.60 (4.32)	3.54 (3.36)
(1, 2, 2)	1.47 (0.89)	1.96 (1.49)	1.91 (1.46)	1.92 (1.47)
(1, 2, 5)	1.00 (0.07)	1.02 (0.13)	1.01 (0.12)	1.02 (0.14)
(2, 1.25, 0.5)	6.32 (7.72)	7.79 (9.22)	6.12 (7.32)	5.49 (6.64)
(2, 1.25, 2)	1.03 (0.20)	1.07 (0.28)	1.07 (0.29)	1.10 (0.38)
(2, 1.25, 5)	1.00 (0.00)	1.00 (0.00)	1.00 (0.01)	1.00 (0.02)
(2, 1.5, 0.5)	6.43 (7.37)	7.26 (7.86)	5.06 (5.42)	4.17 (4.38)
(2, 1.5, 2)	1.04 (0.21)	1.09 (0.33)	1.08 (0.32)	1.11 (0.38)
(2, 1.5, 5)	1.00 (0.00)	1.00 (0.01)	1.00 (0.00)	1.00 (0.02)
(2, 2, 0.5)	6.18 (6.56)	5.51 (5.5)	3.52 (3.24)	2.77 (2.49)
(2, 2, 2)	1.05 (0.24)	1.13 (0.39)	1.11 (0.37)	1.12 (0.38)
(2, 2, 5)	1.00 (0.00)	1.00 (0.02)	1.00 (0.01)	1.00 (0.02)
	Cauchy Distribution			
(0.5, 1.25, 0.5)	53.57 (61.06)	16.33 (18.06)	13.56 (15.43)	14.86 (16.92)
(0.5, 1.25, 2)	14.08 (27.34)	22.93 (47.32)	30.35 (70.55)	32.27 (78.56)
(0.5, 1.25, 5)	1.72 (1.64)	1.95 (2.02)	2.29 (2.81)	2.39 (3.24)
(0.5, 1.5, 0.5)	37.85 (42.48)	12.07 (13.12)	9.76 (10.65)	10.68 (11.88)
(0.5, 1.5, 2)	9.7 (16.37)	15.07 (26.56)	18.9 (39.65)	20.16 (49.68)
(0.5, 1.5, 5)	1.47 (1.13)	1.61 (1.33)	1.81 (1.77)	1.86 (2.04)
(0.5, 2, 0.5)	22.92 (24.58)	7.61 (8.01)	6.17 (6.4)	6.41 (6.74)
(0.5, 2, 2)	5.9 (8.71)	8.44 (12.22)	9.61 (16.26)	10.32 (17.3)
(0.5, 2, 5)	1.23 (0.64)	1.33 (0.78)	1.40 (0.94)	1.45 (1.1)
(1, 1.25, 0.5)	69.54 (77.15)	20.67 (22.66)	16.16 (18.17)	17.31 (19.93)
(1, 1.25, 2)	7.46 (15.32)	10.38 (37.66)	14.63 (38.79)	15.39 (49.03)
(1, 1.25, 5)	1.35 (1.07)	1.4 (1.18)	1.62 (1.74)	1.64 (1.93)
(1, 1.5, 0.5)	49.2 (54.18)	14.78 (15.86)	11.49 (12.66)	12.11 (13.51)
(1, 1.5, 2)	5.52 (9.28)	7.32 (13.4)	9.85 (25.48)	10.5 (27.33)
(1, 1.5, 5)	1.24 (0.82)	1.26 (0.8)	1.40 (1.20)	1.42 (1.3)
(1, 2, 0.5)	28.98 (30.58)	9.07 (9.42)	7.01 (7.26)	7.13 (7.54)
(1, 2, 2)	3.91 (5.14)	4.96 (6.9)	5.92 (10.63)	6.30 (11.66)
(1, 2, 5)	1.12 (0.44)	1.16 (0.52)	1.20 (0.61)	1.23 (0.75)
(2, 1.25, 0.5)	61.93 (83.08)	21.61 (24.4)	15.79 (18.6)	15.20 (19.11)
(2, 1.25, 2)	2.59 (4.52)	2.66 (4.93)	3.91 (12.02)	4.04 (12.51)
(2, 1.25, 5)	1.09 (0.48)	1.06 (0.37)	1.14 (0.68)	1.15 (0.85)
(2, 1.5, 0.5)	48.12 (60.04)	16.59 (18.11)	11.80 (13.31)	11.25 (13.67)
(2, 1.5, 2)	2.27 (3.15)	2.38 (3.69)	3.19 (6.81)	3.34 (8.68)
(2, 1.5, 5)	1.05 (0.32)	1.04 (0.26)	1.09 (0.44)	1.10 (0.59)
(2, 2, 0.5)	31.8 (36.68)	10.61 (11.07)	7.37 (7.87)	6.90 (7.46)
(2, 2, 2)	1.99 (2.14)	2.16 (2.38)	2.53 (3.63)	2.70 (4.35)
(2, 2, 5)	1.03 (0.21)	1.03 (0.19)	1.05 (0.28)	1.06 (0.32)
	Exponential Distribution			
(0.5, 1.25, 0.5)	202.97 (389.94)	466.73 (817.74)	734.88 (1380.12)	808.88 (1656.48)
(0.5, 1.25, 2)	3.08 (3.40)	4.65 (5.71)	5.22 (6.97)	6.5 (10.05)
(0.5, 1.25, 5)	1.09 (0.35)	1.13 (0.43)	1.17 (0.53)	1.28 (0.74)
(0.5, 1.5, 0.5)	69.94 (112.83)	204.2 (317.31)	232.76 (386.76)	226.1 (435.51)
(0.5, 1.5, 2)	1.86 (1.50)	2.61 (2.55)	2.75 (2.81)	3.05 (3.37)
(0.5, 1.5, 5)	1.02 (0.15)	1.04 (0.2)	1.05 (0.24)	1.08 (0.32)
(0.5, 2, 0.5)	19.17 (23.96)	60.24 (79.86)	55.61 (74.09)	48.08 (69.62)
(0.5, 2, 2)	1.24 (0.59)	1.52 (0.98)	1.52 (0.99)	1.55 (1.05)
(0.5, 2, 5)	1.00 (0.03)	1.00 (0.06)	1.00 (0.06)	1.01 (0.08)
(1, 1.25, 0.5)	25.23 (53.44)	64.24 (128.34)	80.3 (190.78)	99.09 (232.2)
(1, 1.25, 2)	1.38 (0.90)	1.56 (1.25)	1.73 (1.56)	2.16 (2.38)
(1, 1.25, 5)	1.01 (0.09)	1.01 (0.09)	1.01 (0.13)	1.04 (0.24)
(1, 1.5, 0.5)	12.08 (18.33)	29.7 (49.51)	34.15 (58.3)	37.13 (67.25)
(1, 1.5, 2)	1.16 (0.48)	1.26 (0.67)	1.34 (0.84)	1.49 (1.07)
(1, 1.5, 5)	1.00 (0.04)	1.00 (0.04)	1.00 (0.05)	1.01 (0.10)
(1, 2, 0.5)	5.24 (6.30)	11.94 (16.32)	12.49 (17.58)	12.06 (16.61)
(1, 2, 2)	1.04 (0.21)	1.08 (0.31)	1.10 (0.36)	1.13 (0.43)

(1, 2, 5)	1.00 (0.00)	1.00 (0.01)	1.00 (0.01)	1.00 (0.02)
(2, 1.25, 0.5)	1.30 (1.00)	1.28 (1.38)	1.57 (2.23)	2.52 (4.44)
(2, 1.25, 2)	1.00 (0.04)	1.00 (0.03)	1.00 (0.06)	1.02 (0.16)
(2, 1.25, 5)	1.00 (0.00)	1.00 (0.00)	1.00 (0.00)	1.00 (0.01)
(2, 1.5, 0.5)	1.20 (0.71)	1.17 (0.73)	1.36 (1.27)	1.88 (2.32)
(2, 1.5, 2)	1.00 (0.02)	1.00 (0.02)	1.00 (0.03)	1.01 (0.09)
(2, 1.5, 5)	1.00 (0.00)	1.00 (0.00)	1.00 (0.00)	1.00 (0.01)
(2, 2, 0.5)	1.10 (0.42)	1.09 (0.46)	1.19 (0.70)	1.44 (1.15)
(2, 2, 2)	1.00 (0.01)	1.00 (0.01)	1.00 (0.01)	1.00 (0.04)
(2, 2, 5)	1.00 (0.00)	1.00 (0.00)	1.00 (0.00)	1.00 (0.00)

5. Application in monitoring arrival delay

In this section, we illustrate the application of the proposed chart to a real problem. We consider arrival delay data of the Trenord railway network in Italy at the Mortara station for the R25 line between the cities of Novara and Mortara (referred to as Direttrice -route- D26). Trenord is a railway company in Italy which is accountable for the operation of regional passenger trains mainly in the northern Italian Lombardy region. Between August 4 and 31, 2019, there was a reduced train schedule for various works on the railways for service improvement. Here, we consider the arrival delay as one of the measures of service quality. There was no service on this route on September 1, 2019, and the service resumed on the next day. In a press release dated October 17 2019, the chief executive officer of Trenord stated that during the previous months of 2019, the service has been markedly improved.

For this reason, we consider arrival delays during the September 02 - October 17, 2019 period for collecting the Phase-I data. In a typical day, there are three trains on the route-D26. There are some days with no service and a few days with reduced service. We consider the 36 days within this period with full service, that is, with all three trains operating in the route and obtain a total of 108 data points. First, we establish whether the 108 observations can be perceived as the Phase-I sample. To this end, the Box-Pierce and Ljung-Box tests for testing the possible presence of autocorrelation is applied. The p-values of both tests for autocorrelation with lag 1 are higher than 0.3. For lag values between 2 to 7, the p-values are even larger. Therefore, there is practical evidence that the sequence of observations is a random sample. Figure 3 displays the histogram and density plot of the Phase-I observations and indicates the possible presence of a few extreme observations. Now, we should identify them, if present, via an appropriate Phase-I control chart.

Figure 3. Histogram and density plot of the Phase-I observations

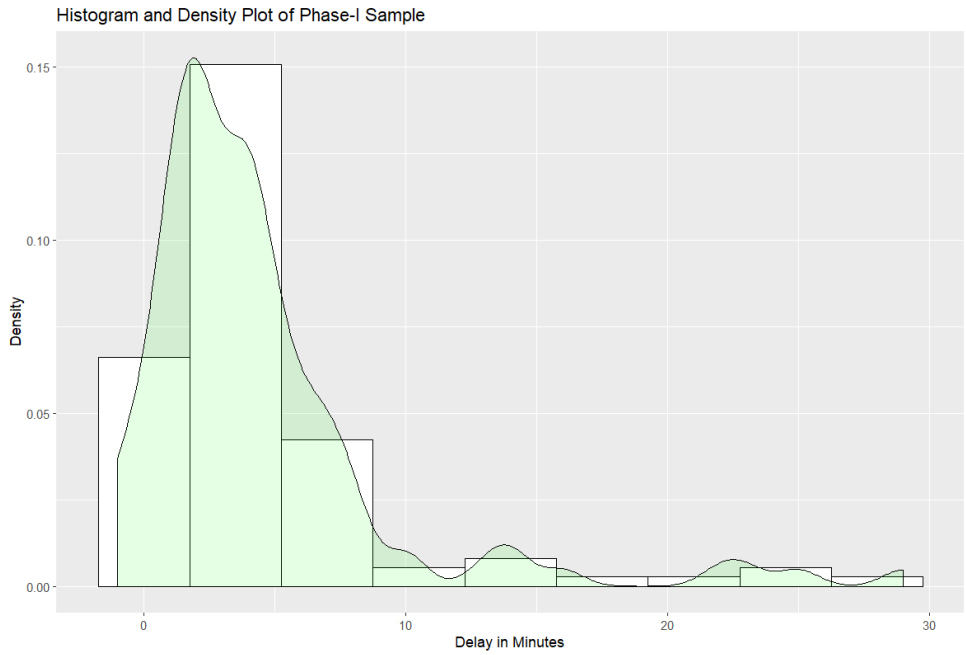

We can check using the Easyfit software that most of the well-known time-to-event distributions, such as two-parameter exponential, Weibull or lognormal do not fit well to these data. Therefore it is recommended a nonparametric Phase-I analysis. It might be preferable and convenient to monitor after every two days of full operations using a subgroup of size 6. Hence, we first apply the RS/P chart for Phase-I analysis, introduced by Capizzi, & Masarotto (2013), over 18 subgroups of size $n = 6$, see Figure 4. The results are consistent with the previous ones since both p-values, respectively for level and scale, are again equal to 1, and the process is deemed to be IC.

Figure 4. Phase-I RS/P control chart for the reference sample observations based on subgroups

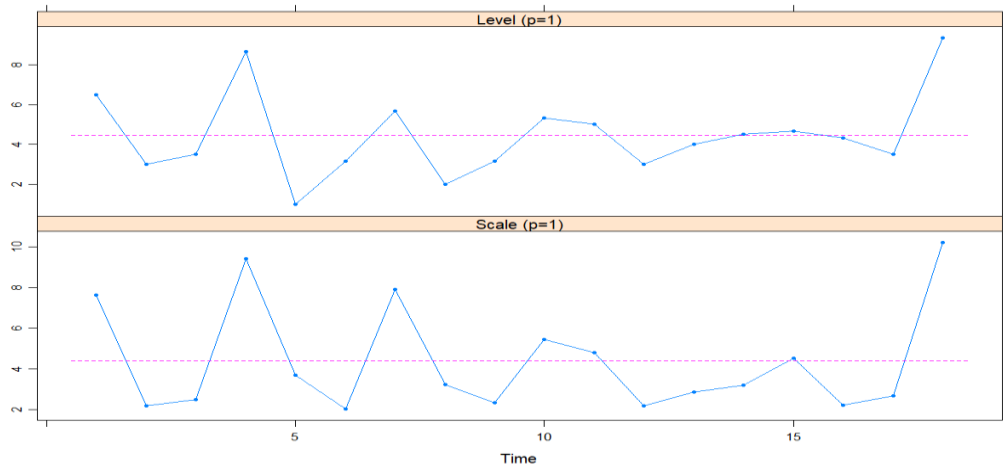

While the RS/P Phase-I chart is excellent for detecting a sustained shift, the Phase-I Lepage chart introduced by Li, Mukherjee, & Su (2019) is known to be more efficient in detecting one or two isolated shifts. In Figure 5, we present the Phase-I Lepage chart setting the false alarm probability at 0.1, for which the control limit is 9.333. The results clearly indicate that the 108 observations may be safely taken as the reference sample.

Figure 5, The Phase-I Lepage chart for the reference sample

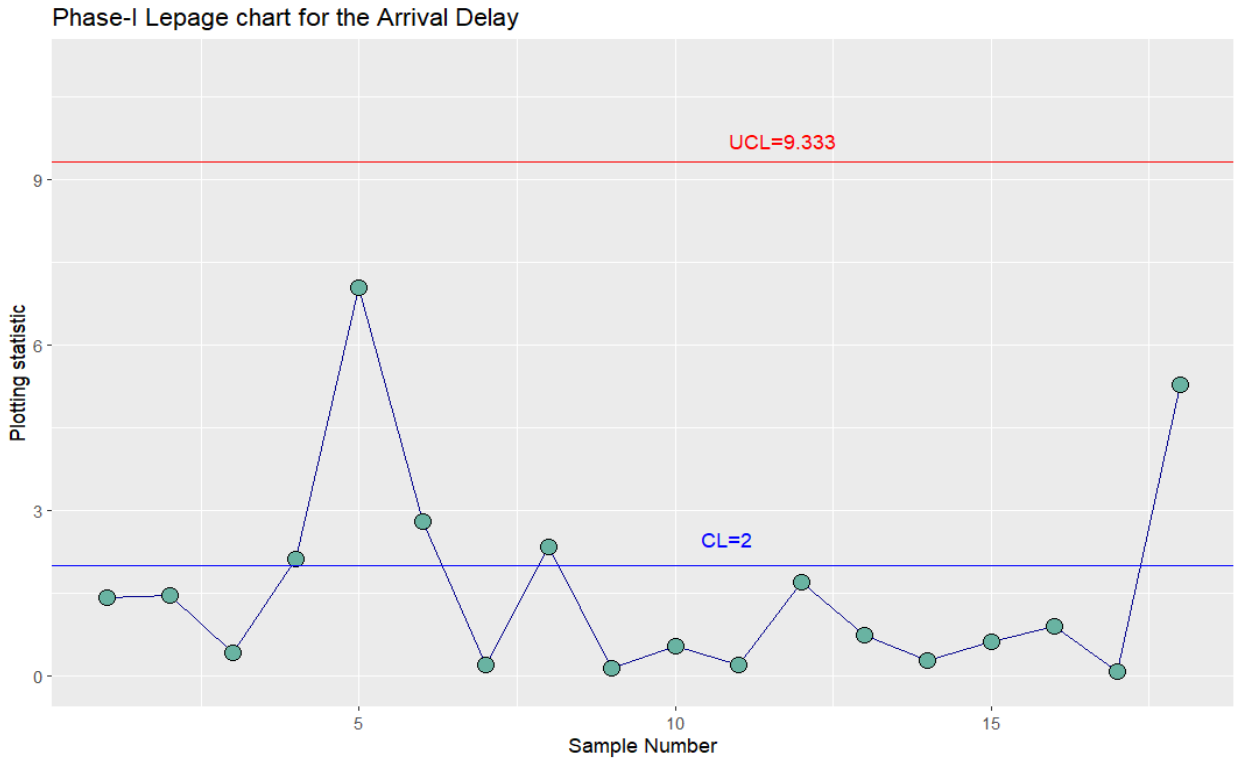

After Phase-I analysis, Phase-II monitoring is planned with the established reference sample to monitor the service quality in terms of delay time. A change in location, scale or shape of the distribution of arrival delay can be detected with the proposed LVS charting scheme. We consider, as before, 6 data points from every second day of full-service operations for the rest of the year. Given (m,n) = (108,6), the UCL (H) for the proposed LVS chart is determined via Monte-Carlo simulations as 17.79 for a target $ARL_0 = 370$. The median line is 1.81. The standardized values of the three statistics behind the proposed chart, namely the Wilcoxon one for location (L), AB for variability (V) and Savage for shape (S), and the plotting statistics for the LVS chart are computed. The results are presented in Table A.1 in the Appendix. We plot the corresponding

observed value of the various statistics against the corresponding sample number in Figure 6. In the same plot, labels L, V, and S are used to distinguish the corresponding location, variability and shape statistics.

From Figure 6, we see that there is a clear OOC signal at test sample number 4. Moreover, there is a run of 10 consecutive samples (from 3 to 12) over the median line. The value of the plotting statistic for sample number 2 falling below the median line just by a margin of 0.01, otherwise, it would have been a run 12 consecutive samples from 1 to 12. We see a similar run of 8 points from sample number 14 to number 21. These are quite clear indications of a shift. To understand which aspect is more responsible for the shift, we can look at the L, V, and S statistics values. Figure 5 shows that the L-component corresponding to all of the first 9 sample points is above the baseline. This is a clear indication of a shift in location. We conclude that the improvement of service quality did not extend to the later months of 2019 in route D26, and further assessment would have been necessary to reduce delay.

Figure 6. Integrated LVS chart with sub-charts for location, scale and shape components for delay data

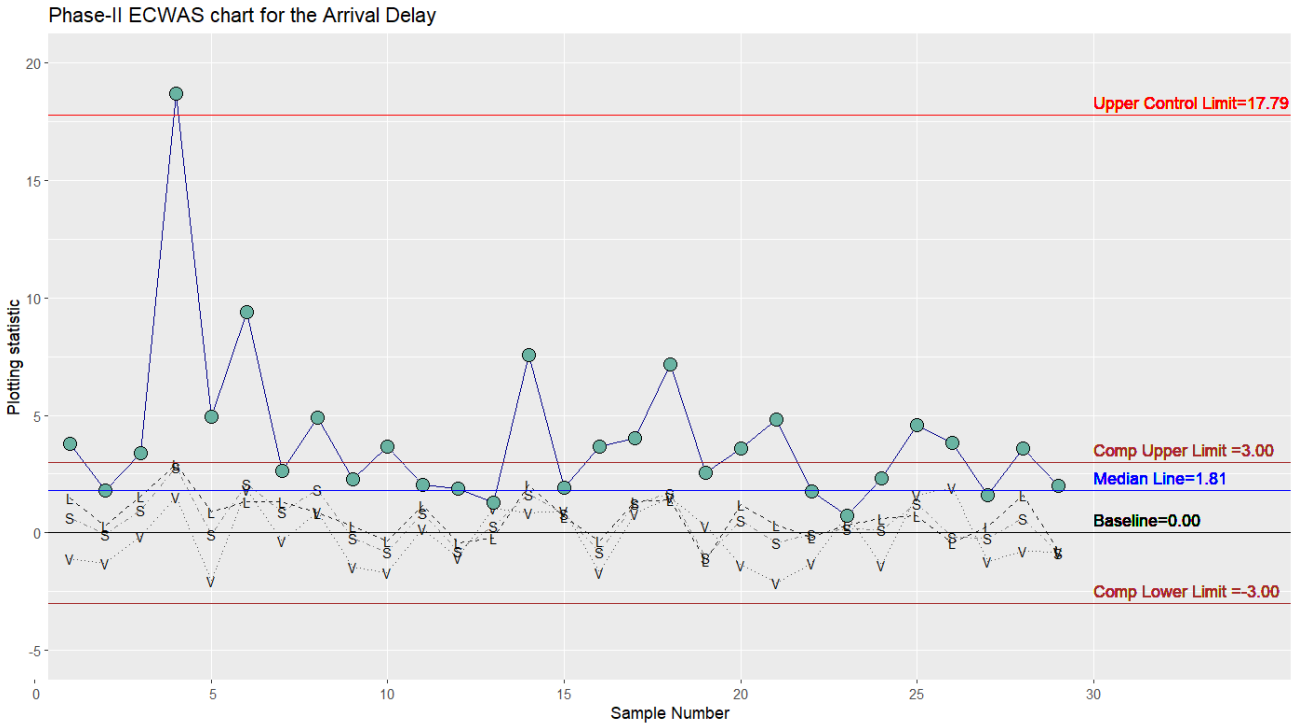

6. Concluding remarks

In this paper, we fill a gap in the literature on distribution-free charting schemes for process monitoring by introducing a new distribution-free process monitoring scheme that can detect a shift in either of location, scale and shape parameters of the process distribution, or any combinations of them. In fact, the available distribution-free charts are either uni-aspect schemes (because they can detect a shift in only one aspect, like location or scale) or bi-aspect schemes (because they can simultaneously detect a shift in location and scale). The new scheme is based on a combined statistic designed via Euclidean distance of the standardized Wilcoxon statistic for location, the standardized Ansari-Bradley statistic for scale and the standardized Savage-type statistic for shape. We discuss the implementation design using the average run-length as a metric and investigate the in-control performance of the proposed scheme. It is shown that the new chart is in-control robust irrespective to the underlying process distribution and therefore applicable to monitor any univariate continuous processes. An out-of-control performance comparison study of the new scheme with many existing schemes shows that the new scheme is preferable to the existing schemes, as none of them is designed to monitor the three process parameters simultaneously. The application of the new chart in monitoring arrival delays of a passenger train in a regional route in Italy shows that the chart is useful in practice to detect the presence of shifts. The chart also allows us to understand which aspect is more responsible for a shift among location, scale and shape. This is a significant advantage of the new chart since it dramatically helps quality engineers in finding out the assignable cause. Possible directions for further research are the CUSUM and EWMA version of the proposed LVS scheme.

References

Abid, M., Nazir, H. Z., Riaz, M., & Lin, Z. (2017). An efficient nonparametric EWMA Wilcoxon signed-rank chart for monitoring location. *Quality and Reliability Engineering International*, 33, 669–685.

Balakrishnan, N., Triantafyllou, I. S., & Koutras, M. V. (2009). Nonparametric control charts based on runs and Wilcoxon-type rank-sum statistics. *Journal of Statistical Planning and Inference*, 139(9), 3177-3192.

Capizzi, G., & Masarotto, G. (2017). Phase I distribution-free analysis of multivariate data. *Technometrics*, 59(4), 484-495.

Celano, G., Castagliola, P., & Chakraborti, S. (2016). Joint Shewhart control charts for location and scale monitoring in finite horizon processes. *Computers & Industrial Engineering*, 101, 427–439.

Chakraborti, S., Eryilmaz, S., & Human, S. W. (2009). A phase II nonparametric control chart based on precedence statistics with runs-type signaling rules. *Computational Statistics and Data Analysis*, 53, 1054–1065.

Chakraborti, S. & Graham, M. (2019). *Nonparametric Methods for Statistical Quality Control*. New York: Wiley.

Chakraborti, S., Van Der Laan, P. & Bakir, S. T. (2001). A phase II nonparametric control chart based on precedence statistics with runs-type signaling rules. *Journal of Quality Technology*, 33, 304–315.

Chong, Z. L., Huang, S., Mukherjee, A., & Yang, J. (2020). Performance comparisons of distribution-free Shewhart-type Lepage and Cucconi schemes in monitoring complex process distributions. *Transactions of the Institute of Measurement and Control* (Sage), Vol. 42(14) 2787–2811.

Chong, Z. L., Mukherjee, A., & Khoo, M. B. C. (2017). Distribution-free Shewhart-Lepage type premier control schemes for simultaneous monitoring of location and scale. *Computers & Industrial Engineering*, 104, 201–215.

Chong, Z. L., Mukherjee, A., & Khoo, M. B. C. (2018). Some distribution-free Lepage–type schemes for simultaneous monitoring of one-sided shifts in location and scale. *Computers & Industrial Engineering*, 115, 653–669.

Chowdhury, S., Mukherjee, A., & Chakraborti, S. (2014). A new distribution-free control chart for joint monitoring of unknown location and scale parameters of continuous distributions. *Quality and Reliability Engineering International*, 30 (2), 191–204.

Chowdhury, S., Mukherjee, A., & Chakraborti, S. (2015). Distribution-free phase II CUSUM control chart for joint monitoring of location and scale. *Quality and Reliability Engineering International*, 31 (1), 135–151.

David, H., & Grigoryan, A. (2006). Joint statistical design of double sampling X and s charts. *European Journal of Operational Research*, 168, 122–142.

Graham, M. A., Chakraborti, S., & Human, S. W. (2011). A nonparametric EWMA sign chart for location based on individual measurements. *Quality Engineering*, 23(3), 227–241.

Graham, M. A., Mukherjee, A., & Chakraborti, S. (2012). Distribution-free exponentially weighted moving average control charts for monitoring unknown location. *Computational Statistics and Data Analysis*, 56, 2539–2561.

Gupta, R. D., & Gupta, R. C. (2008). Analyzing skewed data by power normal model. *Test*, *17*(1), 197-210.

Gupta RC, Gupta PK, Gupta RD. (1998). Modeling failure time data by Lehman alternatives. *Communications in Statistics Theory and Methods*. 27(4), 887-904.

Gupta, R. D., & Kundu, D. (2001). Exponentiated exponential family: an alternative to gamma and Weibull distributions. *Biometrical Journal: Journal of Mathematical Methods in Biosciences*, *43*(1), 117-130.

Hawkins, D. M., & Deng, Q. (2010). A nonparametric change-point control chart. *Journal of Quality Technology*, 42, 165–173.

Hollander, M., Wolfe, D. A. & Chicken, E. (2013). *Nonparametric Statistical Methods, 3rd Edition*. New York: Wiley.

Jones, L. A., & Champ, C. W. (2010). A distribution-free phase I control chart for subgroup scale. *Journal of Quality Technology*, 42, 373–387.

Kössler, W, & Mukherjee, A. (2020). Distribution-free simultaneous tests for location–scale and Lehmann alternative in two-sample problem. *Biometrical Journal*, 62(1), 99-123.

Koutras, M. V., & Triantafyllou, I. S. (2018). A general class of nonparametric control charts. *Quality and Reliability Engineering International*, 34 (3), 427–435.

Koutras, M. V., & Triantafyllou, I. S. (Eds.) (2020). *Distribution-Free Methods for Statistical Process Monitoring and Control*. Cham, Switzerland: Springer International Publishing.

Kundu, D., & Gupta, R. D. (2013). Power-normal distribution. *Statistics*, *47*(1), 110-125.

Lee, P. H. (2013). Joint statistical design of X and s charts with combined double sampling and variable sampling interval. *European Journal of Operational Research*, 225, 285–297.

Lehmann, E. L. (2009). Parametric versus nonparametrics: two alternative methodologies. *Journal of Nonparametric Statistics*, 21, 397-405.

Lepage, Y. (1971). A combination of Wilcoxon's and Ansari-Bradley's statistics. *Biometrika*, 58, 213–217.

Li, C., Mukherjee, A., Su, Q., & Xie, M. (2019). Some monitoring procedures related to asymmetry parameter of Azzalini's Skew-normal model. *REVSTAT–Statistical Journal*, *17*(1), 1-24.

Li, C., Mukherjee, A., & Su, Q. (2019). A distribution-free Phase I monitoring scheme for subgroup location and scale based on the multi-sample Lepage statistic. *Computers & Industrial Engineering*, 129, 259-273

Li, S.-Y., Tang, L. C., & Ng, S. H. (2010). Nonparametric CUSUM and EWMA control charts for detecting mean shifts. *Journal of Quality Technology*, 42, 209–226.

Li, Z., Xie, M., & Zhou, M. (2016). Rank-based EWMA procedure for sequentially detecting changes of process location and variability. *Quality Technology & Quantitative Management*, 15 (3), 354–373.

Marozzi, M. (2013). Nonparametric simultaneous tests for location and scale testing: a comparison of several methods. *Communications in Statistics - Simulation and Computation*, 42 (6),1298–1317.

Mukherjee, A. (2017). Distribution-free phase-II exponentially weighted moving average schemes for joint monitoring of location and scale based on sub-group samples. *The International Journal of Advanced Manufacturing Technology*, 92 (1–4), 101–116.

Mukherjee, A., & Chakraborti, S. (2012). A distribution-free control chart for the joint monitoring of location and scale. *Quality and Reliability Engineering International*, 28, 335–352.

Mukherjee, A., & Marozzi, M. (2017a). Distribution-free Lepage type circular-grid charts for joint monitoring of location and scale parameters of a process. *Quality and Reliability Engineering International*, 33 (2), 241–274.

Mukherjee, A., & Marozzi, M. (2017b). A distribution-free phase-II CUSUM procedure for monitoring service quality. *Total Quality Management & Business Excellence*, 28 (11–12), 1227–1263.

Mukherjee, A., & Sen, R. (2018). Optimal design of Shewhart-Lepage type schemes and its application in monitoring service quality. *European Journal of Operational Research*, 266 (1), 147–167.

Mukherjee, A. & Marozzi, M. (2020): Nonparametric Phase-II control charts for monitoring high-dimensional processes with unknown parameters, *Journal of Quality Technology*, (To Appear) DOI: 10.1080/00224065.2020.1805378

Qiu, P. (2014). *Introduction to Statistical Process Control*. Boca Raton, FL: Chapman & Hall/CRC.

Qiu, P. (2018). Some perspectives on nonparametric statistical process control. *Journal of Quality Technology*, 50 (1), 49–65.

Qiu, P., & Li, Z. (2011). On nonparametric statistical process control of univariate processes. *Technometrics*, 53 (4), 390–405.

Qiu, P., & Zhang, J. (2015). On phase II SPC in cases when normality is invalid. *Quality and Reliability Engineering International*, 31 (1), 27–35.

Rahim, M. A., & Costa, A. F. B. (2000). Joint economic design of X-bar and R charts under Weibull shock models. *International Journal of Production Research*, 38, 2871–2889.

Ross, G. J., & Adams, N. M. (2012). Two nonparametric control charts for detecting arbitrary distribution changes. *Journal of Quality Technology*, 44, 102–116.

Song, Z., Mukherjee, A., Liu, Y., & Zhang, J. (2019). Optimizing joint location-scale monitoring–An adaptive distribution-free approach with minimal loss of information. European Journal of Operational Research, 274(3), 1019-1036.

Song, Z., Mukherjee, A., & Zhang, J. (2020) An efficient approach of designing distribution-free exponentially weighted moving average schemes with dynamic fast initial response for joint monitoring of location and scale, *Journal of Statistical Computation and Simulation*, 90:13, 2329-2353.

Song, Z., Mukherjee, A., & Zhang, J. (2020). Some robust approaches based on copula for monitoring bivariate processes and component-wise assessment. *European Journal of Operational Research*. (To Appear) https://doi.org/10.1016/j.ejor.2020.07.016.

Song, Z., Mukherjee, A., Marozzi, M., & Zhang, J. (2020). A Class of Distribution-Free Exponentially Weighted Moving Average Schemes for Joint Monitoring of Location and Scale Parameters. In Koutras, M. V., & Triantafyllou, I. S. (Eds.) (2020). *Distribution-Free Methods for Statistical Process Monitoring and Control*. Cham, Switzerland: Springer International Publishing, 183-217.

Zhang, J., Li, E., & Li, Z. (2017). A Cramér–von Mises test-based distribution-free control chart for joint monitoring of location and scale. *Computers & Industrial Engineering*, 110, 484–497.

Zhang, W., Yang, M., Khoo, M. B. C., & Yu, F. J. (2010). Optimization designs and performance comparison of two CUSUM schemes for monitoring process shifts in mean and variance. *European Journal of Operational Research*, 205, 136–150.

Zhou, M., Zhou, Q., & Geng, W. (2016). A new nonparametric control chart for monitoring variability. *Quality and Reliability Engineering International*, 32, 2471–2479.

Appendix

Table A.1. Plotting statistic for the proposed *LVS* scheme and the component sub-charts for the delay data

Sample No.	Delay in Minutes	Standardized Wilcoxon (L)	Standardized AB (V)	Standardized Savage (S)	Plotting Statistic T of *LVS* scheme
1	(4, 5, 6, 4, 3, 9)	1.472	-1.091	0.651	3.782
2	(3, 1, 12, 4, 3, 4)	0.298	-1.307	-0.060	1.801
3	(7, 4, 2, 8, 4, 8)	1.561	-0.127	0.962	3.378
4	(8, 21, 14, 5, 5, 9)	2.931	1.523	2.787	18.677
5	(5, 3, 6, 4, 3, 4)	0.869	-2.043	-0.057	4.934
6	(0, 5, 12, 25, 2, 14)	1.326	1.840	2.061	9.394
7	(4, 2, 6, 14, 7, 3)	1.320	-0.355	0.883	2.648
8	(4, 0, 5, 2, 76, 10)	0.857	0.901	1.837	4.920
9	(4, 2, 4, 2, 3, 8)	0.273	-1.459	-0.238	2.261
10	(1, 3, 5, 3, 2, 4)	-0.362	-1.688	-0.826	3.661
11	(1, 3, 4, 9, 6, 10)	1.148	0.190	0.836	2.055
12	(4, 1, 3, 1, 4, 5)	-0.406	-1.041	-0.797	1.883
13	(2, 1, 9, 2, 1, 17)	-0.216	1.066	0.302	1.274
14	(7, 17, 6, 2, 6, 6)	2.043	0.838	1.636	7.551
15	(1, 19, 5, 1, 4, 8)	0.673	0.914	0.796	1.921
16	(3, 1, 5, 3, 2, 4)	-0.362	-1.688	-0.826	3.661
17	(5, 0, 5, 4, 16, 10)	1.339	0.825	1.244	4.021
18	(2, 15, 14, 13, 1, 5)	1.415	1.510	1.696	7.158
19	(0, 0, 3, 4, 1, 6)	-1.161	0.292	-1.064	2.566
20	(7, 3, 9, 4, 4, 3)	1.206	-1.371	0.524	3.606
21	(3, 4, 4, 2, 3, 6)	0.330	-2.132	-0.406	4.820
22	(2, 2, 3, 3, 2, 22)	-0.171	-1.307	-0.074	1.744
23	(4, 1, 6, 5, 10, 0)	0.343	0.761	0.176	0.728
24	(2, 3, 3, 8, 3, 7)	0.628	-1.383	0.124	2.324
25	(22, 2, 10, 0, 2, 10)	0.711	1.599	1.232	4.580
26	(1, 0, 5, 7, -1, 8)	-0.406	1.904	-0.180	3.821
27	(3, 3, 1, 7, 3, 6)	0.266	-1.218	-0.228	1.607
28	(5, 3, 7, 5, 5, 5)	1.618	-0.800	0.593	3.609
29	(7, -1, 2, 3, 3, 2)	-0.755	-0.825	-0.856	1.983